

Unconventional Majorana fermions on the surface of topological superconductors protected by rotational symmetry

Junyeong Ahn^{1,2,3,4,5,*} and Bohm-Jung Yang^{1,2,3,†}

¹*Center for Correlated Electron Systems, Institute for Basic Science (IBS), Seoul 08826, Korea*

²*Department of Physics and Astronomy, Seoul National University, Seoul 08826, Korea*

³*Center for Theoretical Physics (CTP), Seoul National University, Seoul 08826, Korea*

⁴*RIKEN Center for Emergent Matter Science (CEMS), Wako, Saitama 351-0198, Japan*

⁵*Department of Applied Physics, The University of Tokyo, Bunkyo, Tokyo 113-8656, Japan*

(Dated: May 28, 2022)

Topological superconductors are exotic gapped phases of matter hosting Majorana mid-gap states on their boundary. In conventional topological superconductors, Majorana in-gap states appear in the form of either localized zero-dimensional modes or propagating spin-1/2 fermions with a quasi-relativistic dispersion relation. Here we show that unconventional propagating Majorana states can emerge on the surface of three-dimensional topological superconductors protected by rotational symmetry. The unconventional Majorana surface states fall into three different categories: a spin- S Majorana fermion with $(2S + 1)$ -fold degeneracy ($S \geq 3/2$), a Majorana Fermi line carrying two distinct topological charges, and a quartet of spin-1/2 Majorana fermions related by fourfold rotational symmetry. The spectral properties of the first two kinds, which go beyond the conventional spin-1/2 fermions, are unique to topological superconductors and have no counterpart in topological insulators. We show that the unconventional Majorana surface states can be obtained in the superconducting phase of doped Z_2 topological insulators or Dirac semimetals with rotational symmetry.

Topological insulators (TIs) are exotic gapped phases of matter hosting stable gapless fermions on their boundary [1]. One fascinating property of the boundary gapless states in TIs is that they can get around the fermion number doubling theorem. In general, the fermion doubling theorem states that, in periodic systems, a stable gapless fermion carrying quantized topological charges always accompanies its partner with opposite charges, so that the total number of stable gapless fermions should be doubled [2, 3]. For example, the surface of time-reversal-invariant (T -invariant) three-dimensional (3D) TIs can host a single two-dimensional (2D) Dirac fermion with twofold degeneracy at a time-reversal-invariant momentum (TRIM) [4]. Since a single 2D massless Dirac fermion carries a quantized π Berry phase along any loop enclosing it, a 2D periodic system cannot have a single Dirac point with Kramers degeneracy in the Brillouin zone (BZ). However, on the surface of T -symmetric 3D TIs, since the surface Dirac cone can merge with the 3D bulk states, a pair of 2D massless Dirac fermions can separately appear on the top and bottom surfaces, respectively, so that each surface BZ can host a single 2D Dirac fermion with twofold degeneracy and the fermion doubling theorem can be avoided.

Recent progress in the study of topological crystalline insulators (TCIs) [5–26] have shown that various new types of stable gapless fermions protected by crystalline symmetries can appear on their surfaces and evade the relevant fermion doubling theorem enforced by the crystalline symmetries. For instance, a TCI protected by mirror symmetry hosts gapless Dirac fermions on mirror-invariant surfaces [6, 7]. In the case of 3D systems with nonsymmorphic symmetries, a surface with glide mirror symmetry can exhibit so-called hourglass

fermions [8]. Moreover, when the 2D surface symmetry group of nonsymmorphic systems has two intersecting glide lines, a single 2D Dirac point with fourfold degeneracy can appear at a TRIM at the edge of the BZ [9]. Also, it has been recently shown that 3D TCIs with T and discrete n -fold rotation C_n symmetries with $n = 2, 4, 6$ can have n flavors of massless Dirac fermions with twofold degeneracy, whereas any 2D spin-orbit coupled system having these two symmetries must have a multiple of $2n$ Dirac cones, and thus the surface rotation anomaly is realized in these systems [19].

Avoided fermion number multiplication with anomalous surface states can be realized not only in TIs but also in topological superconductors (TSCs). TSCs are another type of gapped phases of matter with exotic gapless surface fermions, called Majorana fermions, which can be roughly described as a half of an ordinary electron. TSCs whose topological properties are protected by crystalline symmetries are called topological crystalline superconductors (TCSCs). In the mean-field description, superconductors are formally equivalent to insulators with additional particle-hole (P) symmetry. Therefore, after properly incorporating P symmetry, the established knowledge of TCIs may also be extended to TCSCs. Significant efforts have been made in this direction to classify bulk topological phases [20–22], understand the bulk-boundary correspondence for Majorana boundary states [23–37], and uncover the relation between the pairing symmetry and the bulk topology [38–44], though there are subtle issues regarding the physical interpretation of the band topology of superconducting phases [43–46].

These preceding works have shown that P symmetry is important for the protection of zero-dimensional (0D) Majorana zero modes in one-dimensional (1D) TSCs, and also in some 2D and 3D TSCs called higher-order TSCs [23–26, 40, 44]. However, in many 2D and 3D TSCs hosting propagating Majorana boundary states, P symmetry is not essential for their topological protection. For example, chi-

* junyeong.ahn@riken.jp

† bjang@snu.ac.kr

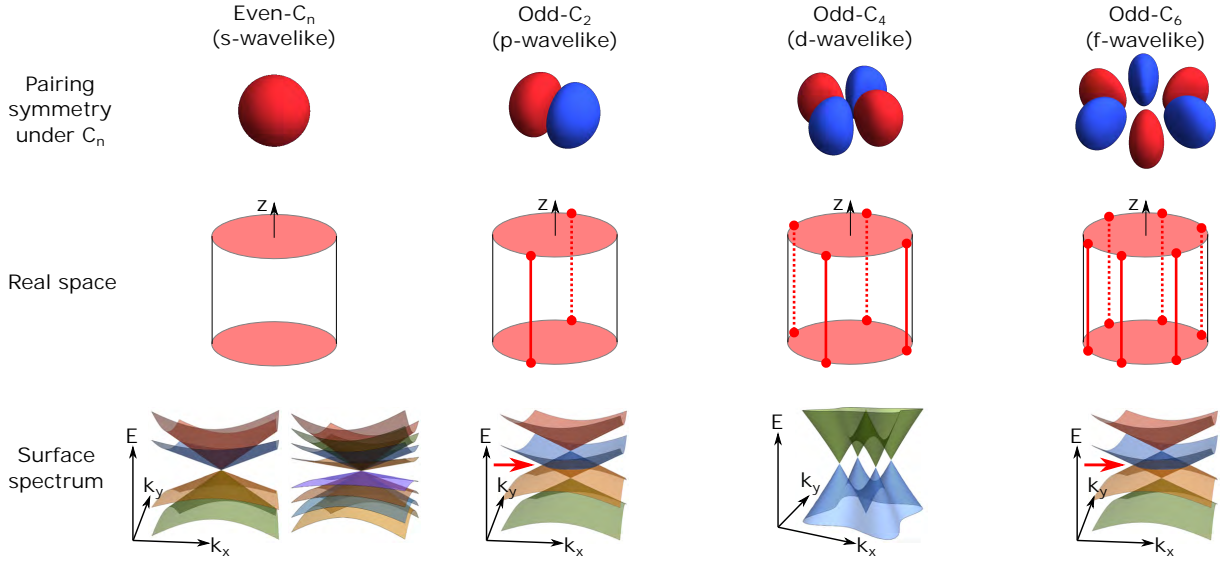


FIG. 1. **Majorana boundary states of rotation-protected topological superconductors.** The top panel shows the symmetry of the pairing function under C_n rotation. The middle shows the real-space geometry of the system. Here, the z -axis is the rotation axis. Red regions host gapless Majorana fermions. In the case of odd- C_n pairing, gapless Majorana hinge states appear on the sides as well as gapless surface states on the top and bottom surfaces. The emergence of Majorana hinge states can be understood from the pairing symmetry of the Cooper pairs, which implies the existence of domain walls on the side surfaces where the pairing gap vanishes. The characteristic surface spectra on C_n -invariant surfaces are shown on the bottom panel. Higher-spin Majorana fermions (HSMFs) appear as anomalous surface states for even- C_n pairing. Spin- S Majorana fermions are characterized by $(2S + 1)$ -fold degenerate Majorana zero modes at a C_n -invariant momentum and linear dispersion relations away from it. Energy spectra for $S = 3/2$ and $S = 7/2$ are shown. For odd- C_2 and odd- C_6 pairing, a doubly charged Majorana Fermi line (DCMFL) appears. The red arrow indicates the zero energy where the Majorana Fermi line exists. In the case of odd- C_4 pairing, a quartet of Majorana fermions (QMF) appears similar to the surface states of rotation-protected topological crystalline insulators [19].

ral edge states in $p_x + ip_y$ superconductors [47] and hour-glass fermions in nonsymmorphic superconductors [34, 35] are similar to the boundary states of quantum anomalous Hall insulators and those of nonsymmorphic TIs, respectively, except that the spectral symmetry between positive and negative energy states is lost in TIs. Instead, there are a few examples of propagating Majorana boundary states which are protected by chiral S symmetry, a combination of T and P symmetries, including multiple helical Majorana surface states protected by S symmetry [48, 49] and Möbius fermions protected by S and nonsymmorphic symmetries [18, 21, 32–35].

One common feature of the propagating Majorana surface states, known up to now, is that they are described by gapless spin-1/2 fermions with a quasi-relativistic dispersion relation, similar to the surface states of TIs or TCIs. However, there is no fundamental reason for the surface states of TSCs or TCSCs to take the form of a spin-1/2 fermion with a quasi-relativistic dispersion relation. Recent discoveries of novel low-energy excitations in bulk semimetals or bulk nodes of superconductors, such as spin-1 and spin-3/2 fermions [50–53], nodal lines [54, 73] and nodal surfaces [56, 57], have shown that novel fermionic excitations protected by crystalline symmetries can emerge in bulk crystals, although none of them has been realized as anomalous surface states. On the surface of TCSCs, the additional P symmetry combined with crystalline symmetries may allow new types of Majorana boundary fermions distinct from spin-1/2 fermions, which are

unique to TSCs and unachievable in TCIs.

Here, we show that unconventional Majorana fermions (MFs) can emerge on the surface of 3D TCSCs protected by C_n and T symmetries. By analyzing all possible realizations of anomalous surface states, we show that rotation-protected TSCs feature three types of anomalous Majorana surface states, two of which exhibit characteristic energy spectra that have no counterpart in TIs. The first type takes the form of *higher-spin Majorana fermions* (HSMFs), which generalize the spin-3/2 fermion in semimetals [50–53], when the superconducting pairing function is invariant under C_n (we call it even- C_n pairing) [see Fig. 1(a,b)]. Since higher-spin states cannot be realized on the boundary of TIs with any wallpaper symmetry group [9], they are unique to TSCs. Furthermore, our HSMF cannot exist in the bulk of isolated 2D nodal superconductors because their protection requires anomalous C_n symmetry representation. On the other hand, when the pairing function changes sign under $C_{n=2,6}$ (we call it odd- $C_{n=2,6}$ pairing), a *doubly charged Majorana Fermi line* (DCMFL), carrying both 0D and 1D topological charges, appears [Fig. 1(c,d)]. While the 0D topological charge indicates the local stability of the DCMFL, the 1D topological charge guarantees its global stability [57], so that the presence of a single DCMFL definitely violates the fermion doubling theorem. Finally, when the pairing function changes its sign under C_4 (odd- C_4 pairing), a quartet of Majorana fermions (QMF) with twofold degeneracy

appears on a C_4 invariant surface. Since a periodic 2D spin-orbit coupled system with C_4 and T symmetries can host only a multiple of eight MFs with twofold degeneracy, the QMF also avoids the fermion multiplication theorem, which corresponds to the superconducting analog of the C_4 rotation anomaly proposed recently in TCIs with C_n and T symmetries [19]. We show that all three types of anomalous surface states can appear when superconductivity emerges in doped \mathbb{Z}_2 TIs or Dirac semimetals with T and C_n symmetries.

Results

Formalism. The mean-field Hamiltonian for superconductors in the Bogoliubov-de Gennes (BdG) formalism is

$$\hat{H} = \frac{1}{2} \sum_{\mathbf{k}} \hat{\Psi}_{\mathbf{k}}^\dagger H_{\text{BdG}}(\mathbf{k}) \hat{\Psi}_{\mathbf{k}},$$

$$H_{\text{BdG}}(\mathbf{k}) = \begin{pmatrix} h(\mathbf{k}) & \Delta(\mathbf{k}) \\ \Delta^\dagger(\mathbf{k}) & -(U_T)^t h^t(-\mathbf{k}) U_T^* \end{pmatrix}, \quad (1)$$

where $\hat{\Psi} \equiv (\hat{c}_{\mathbf{k}}, \hat{T} \hat{c}_{\mathbf{k}}^\dagger \hat{T}^{-1})^t = (\hat{c}_{\mathbf{k}}, \hat{c}_{-\mathbf{k}}^\dagger U_T)^t$ is the Nambu spinor in which $\hat{c}_{\mathbf{k}}, \hat{c}_{\mathbf{k}}^\dagger$ are electron annihilation/creation operators, and U_T is the unitary part of time reversal operator $\mathcal{T} = U_T K$ with complex conjugation operator K . The superscript t denotes the matrix transpose operation. We use calligraphic (italic) symbols to indicate the symmetry operator of the normal state Hamiltonian (BdG Hamiltonian). $h(\mathbf{k})$ is the normal state Hamiltonian, and the superconducting pairing function $\Delta(\mathbf{k})$ satisfies $\Delta(\mathbf{k}) = -U_T \Delta^t(-\mathbf{k}) U_T^*$ due to the Fermi statistics. This BdG Hamiltonian has particle-hole P symmetry $PH_{\text{BdG}}(\mathbf{k})P^{-1} = -H_{\text{BdG}}(-\mathbf{k})$ where

$$P = \begin{pmatrix} 0 & U_T \\ (U_T)^t & 0 \end{pmatrix} K, \quad (2)$$

which satisfies $P^2 = 1$ (see Methods for a realization of $P^2 = -1$ in spin-SU(2)-symmetric systems).

Let us assume that the normal state has C_n symmetry about the z -axis, so that $C_n h(\mathbf{k}) C_n^{-1} = h(R_n \mathbf{k})$, where $R_n \mathbf{k}$ indicates the momentum after C_n rotation of \mathbf{k} . We assume $C_n \mathcal{T} = \mathcal{T} C_n$, which is valid in all physical systems we consider. When $\Delta(\mathbf{k})$ is an eigenfunction of C_n , i.e., $C_n \Delta(\mathbf{k}) C_n^{-1} = \lambda \Delta(R_n \mathbf{k})$, H_{BdG} is symmetric under $C_n \equiv \text{diag}[C_n, \lambda C_n]$ which satisfies $C_n P = \lambda P C_n$. Namely, $C_n H_{\text{BdG}}(\mathbf{k}) C_n^{-1} = H_{\text{BdG}}(R_n \mathbf{k})$.

Now we suppose that the normal state has time reversal T symmetry $(U_T)^t h^t(-\mathbf{k}) U_T^* = h(\mathbf{k})$. When the superconducting pairing is time-reversal-symmetric, i.e., $\mathcal{T} \Delta(\mathbf{k}) \mathcal{T}^{-1} = \Delta(-\mathbf{k})$, the BdG Hamiltonian is symmetric under $T = \text{diag}(\mathcal{T}, \mathcal{T})$. The consistency with C_n invariance requires $\lambda = \lambda^*$ for \mathcal{T} -preserving pairing, because $C_n \Delta(\mathbf{k}) C_n^{-1} = C_n \mathcal{T}^{-1} \Delta(-\mathbf{k}) \mathcal{T} C_n^{-1} = \lambda^* \mathcal{T}^{-1} \Delta(-R_n \mathbf{k}) \mathcal{T} = \lambda^* \Delta(R_n \mathbf{k})$. Accordingly, $C_n P = \pm P C_n$ in T -symmetric superconductors, where $\lambda = +1$ and -1 indicate even- C_n pairing and odd- C_n pairing, respectively. For our analysis below, it is convenient to define the chiral symmetry operator $S = i^{s_T + s_P} T P$ satisfying $C_n S = \pm S C_n$ and $S^2 = 1$, where $T^2 = (-1)^{s_T}$ and $P^2 = (-1)^{s_P}$. The commutation relations shown here

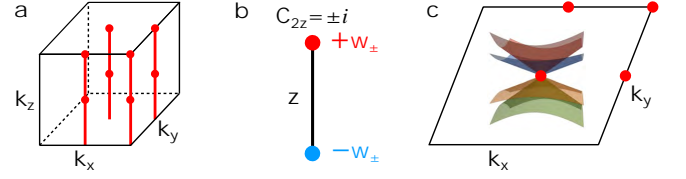


FIG. 2. Bulk topology and surface higher-spin Majorana fermion. **a.** C_{2z} -invariant lines in the 3D Brillouin zone, which are located at $(k_x, k_y) = (0, 0)$, $(\pi, 0)$, $(0, \pi)$, and (π, π) , respectively. **b.** The 1D winding number and chirality of edge states in a C_2 -invariant line. When the winding numbers w_{\pm} in the C_2 eigensector with eigenvalues $\pm i$ are nonzero, $|w_{\pm}|$ Majorana zero modes appear at both edges. The sum of the chirality (the eigenvalue of the chiral operator S) of the zero modes is $+w_{\pm}$ on one edge and $-w_{\pm}$ on the other edge. **c.** Spin-3/2 fermion appearing at $(k_x, k_y) = (0, 0)$ of a C_2 -symmetric surface Brillouin zone. Its fourfold degeneracy originates from the nontrivial winding numbers $w_+ = -w_- = \pm 2$ of the line at $(k_x, k_y) = (0, 0)$.

are generally valid independent of basis choice.

Higher-spin Majorana fermions (HSMFs). Let us first consider the anomalous surface states of TSCs with even- C_n pairing characterized by the relation $C_n P = P C_n$. For convenience, we focus on C_2 -symmetric spin-orbit coupled systems with T symmetry ($C_2^2 = T^2 = -1$) while similar surface states can also appear in other symmetry classes as long as $C_n P = P C_n$ is satisfied [see Supplementary Note (SN)]. The cases with even- $C_{3,4,6}$ pairing are briefly discussed after describing even- C_2 pairing.

On a C_2 -invariant surface, the simplest form of surface states is twofold degenerate MFs with a linear dispersion relation protected by chiral symmetry $S = iTP$. More explicitly, when we take the representation $S = \sigma_z$ and $T = i\sigma_y K$ with Pauli matrices $\sigma_{x,y,z}$, a Majorana surface state can be described by the Hamiltonian $H_s(k_x, k_y) = v_x k_x \sigma_x + v_y k_y \sigma_y$, which carries a winding number $w = \text{sgn}(v_x v_y) = \pm 1$, where $w = (i/4\pi) \oint_{\ell} d\mathbf{k} \cdot \text{Tr} [S H_s^{-1} \nabla_{\mathbf{k}} H_s]$ defined along a loop ℓ surrounding the node at $\mathbf{k} = 0$. The total winding number of surface MFs protected by chiral symmetry gives an integer classification represented by $\mathbb{Z}_{U(1)}$, which is robust independent of the presence of C_2 symmetry.

To observe anomalous surface states that require C_2 symmetry for their protection, let us consider a four-band surface Hamiltonian describing two overlapping MFs with opposite winding numbers: $H_s(k_x, k_y) = k_x \sigma_x + k_y \rho_z \sigma_y$, which is invariant under $S = \sigma_z$ and $T = i\sigma_y K$. Then, possible C_2 representations commuting with S and T , and satisfying $(C_2)^2 = -1$ are $C_2 = -i\rho_z \sigma_z$ and $C_2 = -i\sigma_z = -iS$. In the former case, a mass term $m\rho_y \sigma_y$ opens the gap on the surface. On the other hand, in the latter case, no mass term is allowed, and thus the gapless spectrum is protected. In fact, the fourfold degeneracy at $\mathbf{k} = 0$ is enforced by the representation $C_2 = \pm iS$ because

$$H_s(\mathbf{k}) = -S H_s(\mathbf{k}) S^{-1} = -C_2 H_s(\mathbf{k}) C_2^{-1} = -H_s(-\mathbf{k}), \quad (3)$$

so that $H_s(\mathbf{k} = 0) = 0$. This kind of symmetry-enforced de-

generacy is possible only on the surface of a TSC because $C_2 = \pm iS$ is an anomalous representation that mixes the particle-hole indices, which is impossible in an ordinary C_2 representation of the bulk states. If C_2 symmetry is absent, two zero-energy states with opposite chirality $S = \pm 1$ at $\mathbf{k} = 0$ can be hybridized and shifted away from zero energy, because only the total chirality of zero-energy states is protected by chiral symmetry. In our case, however, two zero-energy states with opposite chiralities have different C_2 eigenvalues, so they are not hybridized at $\mathbf{k} = 0$.

The fourfold degenerate point disperses like spin-3/2 fermions [50–53] because the degeneracy is lifted away from the C_2 -invariant momentum $\mathbf{k} = 0$. In fact, the representation $C_2 = \pm iS$ can generally protect $2n$ -fold degenerate points with an arbitrary natural number n , which we call spin- $(2n - 1)/2$ Majorana fermions (or generally HSMFs). Combined with the total winding number, this integer-valued degeneracy indicates a $\mathbb{Z}_{U(1)} \times \mathbb{Z}_{\text{HS}}$ classification of the surface anomaly, which is consistent with the $\mathbb{Z} \times \mathbb{Z}$ classification of the bulk topology from K-theory [20, 22, 58].

We can understand the corresponding 3D bulk topology of H_{BdG} using the 1D topology on C_2 -invariant lines [Fig. 2(a)], as shown in Ref. [59]. From this, the origin of the anomalous representation $C_2 = \pm iS$ on the surface can be found. Let us recall that, in 1D systems with a winding number w , w zero modes with positive (negative) chirality appear on one (the other) edge [60, 61] [see Fig. 2(b)]. On C_2 -invariant lines, the winding numbers w_{\pm} can be defined in two distinct sectors with C_2 eigenvalues $\pm i$, respectively. When the total winding number $w = w_+ + w_-$ along the z -direction is nontrivial on a C_2 -invariant line, any 1D line parallel to it takes the same w value because w is protected by chiral symmetry that is momentum independent. In other words, w along the z -direction describes the 1D topology of the system. Since we are interested in 3D topology, we consider the case with $w_+ + w_- = 0$, which is automatically satisfied in our system due to time reversal symmetry [See SN]. In this case, $w_+ = -w_- \in \mathbb{Z}$ is the remaining invariant on a C_2 -invariant line, which naturally leads to the anomalous representation $C_2 = \pm iS$ at its edge. Namely, the edge zero modes with opposite C_2 eigenvalues have opposite chiralities. This guarantees the protection of degeneracies at the C_2 -invariant momentum on top and bottom surfaces, as shown in Fig. 2(c). Since the total winding number is zero, the degeneracy at zero energy is lifted away from the C_2 -invariant momentum.

Similarly, HSMFs in TSCs with even- $C_{n=3,4,6}$ pairing can be protected by the 1D winding number defined in each C_n eigensector. To explain the general ideas of the classification of 1D lines [59], let us first suppose that we have only chiral and C_n symmetries. Apart from the total winding number, which is irrelevant to the 3D topological phase, one can find $(n - 1)$ independent winding numbers associated with C_n eigensectors. They give a $\mathbb{Z}_{\text{HS}}^{(n-1)}$ classification of C_n invariant TSCs with chiral symmetry. Additional time reversal and particle-hole symmetries reduce the number of independent winding numbers, leading to different classification [See SN]. For example, for even- C_3 pairing, one can find three winding numbers w_1 , w_2 , and w_3 associated with three

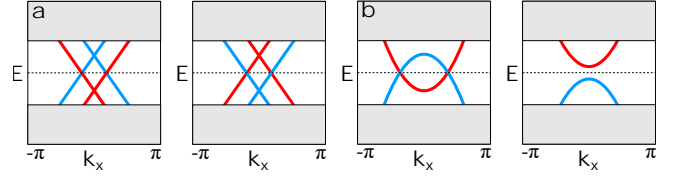


FIG. 3. **Single Majorana Fermi line on a C_2 -invariant surface of superconductors with odd- C_2 pairing.** Shaded regions indicate the bulk energy spectrum of the BdG Hamiltonian in the superconducting state. Red and blue lines originate from the electron and hole surface bands, respectively. The spectrum is shown along the k_x direction, but the spectrum looks alike along the k_y direction. **a.** Surface band structure around a DCMFL. A single DCMFL cannot be annihilated due to the nontrivial 1D topological charge. **b.** Surface band structure around a Majorana Fermi line with a trivial 1D charge. This Majorana Fermi line can be annihilated via a continuous deformation.

C_3 eigenvalues $\{\lambda_1, \lambda_2, \lambda_3\} = \{e^{\pi i/3}, e^{3\pi i/3}, e^{5\pi i/3}\}$ in spin-orbit coupled systems. After excluding the total winding number $w = w_1 + w_2 + w_3$, we have two independent winding numbers that give a \mathbb{Z}_{HS}^2 classification. Additional time reversal symmetry leaves only one independent winding number, leading to a \mathbb{Z}_{HS} classification. A similar consideration gives a full classification of anomalous Majorana surface states with even- C_n pairing, as summarized in Table I. We note that in the case of odd- C_4 and odd- C_6 pairings, the pairing function is also even in C_2 and C_3 , respectively, so that 1D winding numbers are expected to be well defined. However, one can show that, in these cases, C_4 and C_6 symmetries make the 1D winding number in each $C_{n=4,6}$ eigensector be zero [see Methods], and thus HSMFs are not allowed for odd- C_n pairing.

Doubly charged Majorana Fermi lines (DCMFLs). Next we consider the case of odd- C_2 pairing characterized by $C_2S = -SC_2$ (from $C_2P = -PC_2$ and $C_2T = TC_2$), which is incompatible with the representation $C_2 = \pm iS$. In this case, the surface states are protected by C_2T and C_2P symmetries, which do not change the surface momentum $\mathbf{k} = (k_x, k_y)$. Again we first consider time-reversal-symmetric systems with spin-orbit coupling ($C_2^2 = T^2 = -1$) and discuss other cases afterwards. It has been recently shown that 2D systems with the \mathbf{k} -local symmetries satisfying $(C_2T)^2 = (C_2P)^2 = 1$ can host doubly charged nodal lines carrying both 0D and 1D charges [57]. Due to the fermion doubling theorem [2, 3] related to the nontrivial 1D charge, doubly charged nodal lines always appear in pairs in 2D Brillouin zone. However, a C_2 invariant surface of TSCs with odd- C_2 pairing can host an odd number of doubly charged nodal lines, which manifests the C_2 rotation anomaly on the surface. We call this anomalous surface state a DCMFL.

One convenient way of understanding DCMFL is to consider the superconducting instability of a Dirac fermion on the surface of TIs [see Fig. 3(a)]. Let us suppose that a Dirac fermion on a C_2 -invariant surface of a TI is described by the Hamiltonian $h = -\mu + k_x\sigma_x + k_y\sigma_y$ invariant under $C_2 = -i\sigma_z$ and $\mathcal{T} = i\sigma_y K$. Then, there is a unique odd- C_2

pairing function $\Delta(k_x, k_y) = [\Delta \cdot \mathbf{k} + O(k^3)]\sigma_z$ that gives the following surface BdG Hamiltonian

$$H_{\text{BdG}}(k_x, k_y) = k_x \tau_z \sigma_x + k_y \tau_z \sigma_y + \mu \tau_z + \Delta \cdot \mathbf{k} \tau_x \sigma_z, \quad (4)$$

which is symmetric under $C_2 = -i\tau_z \sigma_z$, $T = i\sigma_y K$, and $P = \tau_y \sigma_y K$ where $\tau_{x,y,z}$ are the Pauli matrices for particle-hole indices. In contrast to the case of even- C_2 pairing, there is no anomalous C_2 representation that mixes particle-hole indices, compatible with T and P symmetries. Since the pairing term commutes with \mathbf{k} -linear terms, it does not open a gap at zero energy. Instead, a DCMFL appears along $|\mathbf{k}| = \sqrt{\mu^2 + (\Delta_0 \cdot \mathbf{k})^2}$. The corresponding band structure depicted in Fig. 3 (a) shows its multi-band nature.

The stability of a DCMFL can be understood as follows. If we choose a basis in which $S = \text{diag}[1_{N \times N}, -1_{N \times N}]$ and $C_2 T = K$ where $1_{N \times N}$ denotes the $N \times N$ identity matrix, the surface BdG Hamiltonian takes the following off-diagonal form due to $S H_{\text{BdG}}(\mathbf{k}) + H_{\text{BdG}}(\mathbf{k}) S = 0$:

$$H_{\text{BdG}}(\mathbf{k}) = \begin{pmatrix} 0 & O(\mathbf{k}) \\ O^\dagger(\mathbf{k}) & 0 \end{pmatrix}, \quad (5)$$

where $O(\mathbf{k})$ is real-valued because of $C_2 T = K$ symmetry, so that it can be continuously deformed to an element of the orthogonal group $O(N)$ without closing the band gap. The 0D and 1D topological charges of Majorana Fermi lines are given by the zeroth and first homotopy classes of $O(\mathbf{k})$, which are $\pi_0[O(N)] = \pi_1[O(N)] = \mathbb{Z}_2$ when $N \geq 3$ while $\pi_0[O(N)] = \pi_1[O(N)] = \mathbb{Z}$ when $N = 2$ [37, 57]. Considering that $O(\mathbf{k})$ corresponds to the normal-state Hamiltonian $h(\mathbf{k})$ when $\Delta = 0$, one can see that the topological charges of the Majorana Fermi line (mod 2) originate from the corresponding topological charges of the Fermi lines in the normal state in the weak pairing case. While the 0D charge indicates the local stability of a Majorana Fermi line, its global stability is not guaranteed. For instance, a nodal line that carries a non-trivial 0D charge and a trivial 1D charge is shown in Fig 3(b) where a continuous deformation of the band structure can give a gapped energy spectrum. On the other hand, in the case of a DCMFL shown in Fig 3(a), a continuous deformation of the band structure can merely change the size of the nodal line and the energy spectrum is always gapless. The global stability of a DCMFL is guaranteed by its 1D topological charge, which originates from the π -Berry phase of the normal state Dirac fermion. We note that a single DCMFL cannot be realized when $T^2 = +1$ because the normal state cannot host a single Dirac fermion on the surface (see Methods).

When a DCMFL is realized by odd- $C_{n=2,6}$ pairing, it accompanies gapless hinge states between side surfaces, as shown in the middle panel of Fig. 1. Those hinge states can be understood from the p -wavelike (for odd- C_2 pairing) or f -wavelike (for odd- C_6 pairing) symmetry of the pairing function in real space: when the pairing function changes sign on the side surfaces, there appear gapless hinge states as domain wall states. See Methods for details. The appearance of hinge states on the side surfaces and 2D gapless states on the top and bottom surfaces is similar to the overall surface

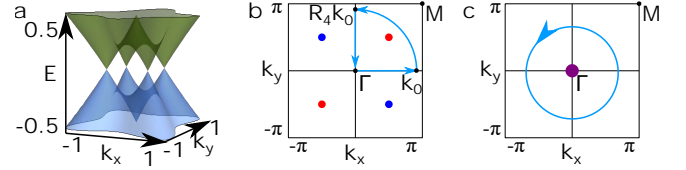


FIG. 4. **A quartet of Majorana fermions (QMF) for odd- C_{4z} pairing.** **a.** Energy spectrum of the BdG Hamiltonian in Eq. (6) with $\mu = 0.5$, $\Delta_1 = 0$, $\Delta_2 = 0.5k_x$, $\Delta_3 = -0.5k_y$ on a C_{4z} invariant surface. **b.** Generic configuration of Majorana fermions in the surface Brillouin zone. Red (blue) dots indicate Majorana fermions with the winding number $+1$ (-1). The Berry phase calculated over the closed trajectory connected by blue arrows characterizes the surface anomaly. **c.** Four Majorana fermions merged at the Γ point. Their global stability is guaranteed by the topological charge Q_4 in Eq. (8) defined along the circle (light blue) enclosing the Γ point.

state structures of TCIs with surface rotation anomaly [19], although the nature of gapless fermions on the top and bottom surfaces is quite different.

Quartet of Majorana fermions (QMF). In the case of odd- C_4 pairing, a quartet of MFs, each with twofold degeneracy, appears on a C_4 invariant surface, as in the case of TCIs with C_4 and T symmetries proposed recently [19]. To understand the origin of the QMF, let us again consider the surface Dirac cone of a T -invariant Z_2 TI, which can be described by the Hamiltonian $h = -\mu + k_x \sigma_x + k_y \sigma_y$. The corresponding BdG Hamiltonian is

$$H_{\text{BdG}} = -\mu \tau_z + k_x \tau_z \sigma_x + k_y \tau_z \sigma_y + \delta H_\Delta, \quad (6)$$

where δH_Δ describes superconducting pairing. Before δH_Δ is introduced, H_{BdG} is composed of two MFs with opposite chiralities (defined with respect to $S = \tau_y$) and has $S = \tau_y$ and $T = i\sigma_y K$ symmetries. There are two possible C_4 representations for odd- C_4 pairing: $C_{4z} = i\tau_x \sigma_z e^{-i\frac{\pi}{4}\sigma_z}$ and $C_{4z} = \tau_z e^{-i\frac{\pi}{4}\sigma_z}$. Here, the former representation is anomalous because it mixes particle-hole indices, but we consider it because surface states might develop an anomalous symmetry representation as in the case of HSMFs. In both cases, the pairing term has the form

$$\delta H_\Delta = \Delta_1(\mathbf{k}) \tau_x + \Delta_2(\mathbf{k}) \tau_x \sigma_x + \Delta_3(\mathbf{k}) \tau_x \sigma_y, \quad (7)$$

where $\Delta_1 \tau_x$ term is a potential mass term that anticommutes with the Dirac Hamiltonian $\tau_z \otimes h$. The representation $C_{4z} = i\tau_x \sigma_z e^{-i\frac{\pi}{4}\sigma_z}$ allows a mass term $\Delta_1 = m$, thus giving trivial surface states. On the other hand, $C_{4z} = \tau_z e^{-i\frac{\pi}{4}\sigma_z}$ forbids such a constant mass term because it requires that Δ_1 has d -wave symmetry: $\Delta_1(-\mathbf{k}) = \Delta_1(\mathbf{k})$ and $\Delta_1(R_4 \mathbf{k}) = -\Delta_1(\mathbf{k})$. In this case, pairing terms split the fourfold degeneracy at $\mathbf{k} = \mathbf{0}$ into four MFs with twofold degeneracy, as shown in Fig. 4(a).

In contrast to the cases of HSMFs and DCMFLs, P symmetry does not play a critical role for the protection of QMF since a similar surface structure can appear in TCIs [19]. When C_4 and T symmetries exist in an isolated 2D lattice system, the total Berry phase of a quadrant of BZ should be zero (mod

AZ class	$(C_n)^n$	T^2	P^2	S^2	even- C_2	even- C_3	even- C_4	even- C_6	odd- $C_{n=2,6}$	odd- C_4	complex- C_n
DIII	-1	-1	1	1	$\mathbb{Z}_{U(1)} \times \mathbb{Z}_{\text{HS}}$	$\mathbb{Z}_{U(1)} \times \mathbb{Z}_{\text{HS}}$	$\mathbb{Z}_{U(1)} \times \mathbb{Z}_{\text{HS}}^2$	$\mathbb{Z}_{U(1)} \times \mathbb{Z}_{\text{HS}}^3$	$(\mathbb{Z}_2)_{\text{DC}}$	$(\mathbb{Z}_2)_{\text{Q}}$	0
CI	1	1	-1	1	$2\mathbb{Z}_{U(1)}$	$2\mathbb{Z}_{U(1)} \times \mathbb{Z}_{\text{HS}}$	$2\mathbb{Z}_{U(1)} \times \mathbb{Z}_{\text{HS}}$	$2\mathbb{Z}_{U(1)} \times \mathbb{Z}_{\text{HS}}^2$	0	0	0
BDI	1	1	1	1	\mathbb{Z}_{HS}	\mathbb{Z}_{HS}	\mathbb{Z}_{HS}^2	\mathbb{Z}_{HS}^3	0	0	0
C or D	± 1	0	± 1	0	0	0	0	0	0	0	0
AIII	± 1	0	0	1	$\mathbb{Z}_{U(1)} \times \mathbb{Z}_{\text{HS}}$	$\mathbb{Z}_{U(1)} \times \mathbb{Z}_{\text{HS}}^2$	$\mathbb{Z}_{U(1)} \times \mathbb{Z}_{\text{HS}}^3$	$\mathbb{Z}_{U(1)} \times \mathbb{Z}_{\text{HS}}^5$	0	0	0

TABLE I. **Classification table for anomalous Majorana surface states in C_n -symmetric 3D superconductors.** T , P , and S represent time reversal, particle-hole, and chiral symmetries, respectively, used for Altland-Zirnbaur (AZ) symmetry classification. AZ classes DIII, CI, and BDI are realized by superconducting pairing in spin-orbit coupled systems, spin-SU(2)-symmetric systems, and spin-polarized systems without spin-orbit coupling, respectively. In spin-polarized systems, the rotation axis is parallel to the spin order. We assume $C_n T = T C_n$ and define T and P such that $T P = P T$. Here, the superconducting pairing function is an eigenfunction of C_n : $C_n \Delta(\mathbf{k}) C_n^{-1} = \lambda \Delta(R_n \mathbf{k})$, where C_n is the matrix representation of C_n for the Bloch state in the normal state, and R_n is the natural action of C_n on momentum. It corresponds to the commutation relation $C_n P = \lambda P C_n$. Even- and odd- C_n pairings correspond to $\lambda = +1$ and $\lambda = -1$, respectively, and complex- C_n pairing indicates that λ is complex-valued. The subscript U(1) indicates that it is the 3D winding number of the Hamiltonian protected by chiral S symmetry. The subscripts HS, DC, and Q indicate that they are responsible for the protection of higher-spin Majorana fermions (HSMFs), doubly charged Majorana Fermi lines (DCMFLs), and a quartet of Majorana fermions (QMF), respectively, on the C_n -preserving surfaces. When time reversal symmetry is broken, there is no 3D topological superconductor protected by C_n symmetry. In class AIII, even-, odd-, and complex- C_n indicate the commutation relation $C_n S = \lambda S C_n$ instead of $C_n P = \lambda P C_n$. Even- C_n TSCs in class AIII systems can be realized in T -symmetric superconductors with spin-orbit coupling and the conservation of the spin z -component [62], where time reversal acts like a chiral operator. Our classification is consistent with the classification of bulk topology in Refs. [20, 22, 58, 59] when there is overlap.

2π) [19]. Since a MF carries a π Berry phase, each quadrant of the BZ should have an even number of MFs so that the total number of MFs should be a multiple of eight. Therefore, the existence of QMF is anomalous and is achievable only on the surface of topological phases [19].

It is worth noting that, while the presence of S symmetry promotes the \mathbb{Z}_2 -valued Berry phase of a twofold degenerate MF to the integer-valued winding number, the global stability of MFs still has a \mathbb{Z}_2 character. To understand this, let us suppose that there are eight MFs on the surface BZ so that a quadrant of the BZ has two MFs with the same chirality. Since the operation of C_4 changes the sign of the winding number for odd- C_4 pairing (See Methods), MFs in the adjacent quadrants should have an opposite sign of winding numbers. Then, by continuously shifting the positions of MFs while keeping T , S , and C_4 symmetries, we can annihilate MFs pairwise at the borders between neighboring quadrants of the BZ. On the other hand, when the number of MFs on the surface is four, such a pair-annihilation process is impossible, and thus QMF is stable. This means that the topological charge associated with the global stability of MFs is related to the parity of the winding number of MFs in a BZ quadrant, which is nothing but the Berry phase.

A more careful consideration, however, shows that the Berry phase itself cannot explain the global stability of QMF. To determine the stability of MFs, one can consider the Berry phase $\Phi_{1/4}^{\mathbf{k}_0}$ computed along the path $\Gamma \rightarrow \mathbf{k}_0 \rightarrow R_4 \mathbf{k}_0 \rightarrow \Gamma$ enclosing a quarter of MFs as shown in Fig. 4(b), where \mathbf{k}_0 indicates an arbitrary momentum, and $\Gamma = (0, 0)$. While $\Phi_{1/4}^{\mathbf{k}_0}$ captures the local stability of MFs located at generic momenta enclosed by the path, it is not well-defined in a special situation where all MFs are merged at a C_{4z} -invariant momentum, say Γ point for convenience, as shown in Fig. 4(c). To confirm the stability of MFs in this situation, we need a topological invariant defined on a circle surrounding Γ point. As shown in

Methods, their \mathbb{Z}_2 topological charge takes the following form

$$Q_4 = \frac{i}{\pi} \log \det D(\mathbf{k}_0) + \frac{1}{\pi} \int_{\mathbf{k}_0}^{R_4 \mathbf{k}_0} d\mathbf{k} \cdot A(\mathbf{k}), \quad (8)$$

where $A(\mathbf{k}) = \sum_{n \in \text{occ}} \langle u_{n\mathbf{k}} | \nabla_{\mathbf{k}} | u_{n\mathbf{k}} \rangle$ is the abelian Berry connection in which occ and $u_{n\mathbf{k}}$ denote the occupied bands and the eigenstates of the BdG Hamiltonian, respectively. $D_{mn}(\mathbf{k}) = \langle u_{mR_n \mathbf{k}} | C_n | u_{n\mathbf{k}} \rangle$ indicates a matrix element of C_n operator. Q_4 is independent of the initial point \mathbf{k}_0 on the loop. While Q_4 can take any value (modulo two, due to the logarithm) in general, it is quantized when additional time reversal symmetry is there. One way to see its \mathbb{Z}_2 quantization is to take a real gauge where $C_{2z} T | u_{n\mathbf{k}} \rangle = | u_{n\mathbf{k}} \rangle$. In this gauge, the abelian Berry connection vanishes, and $\det D = \pm 1$ because D is an orthogonal matrix. Hence $Q_4 = 0$ or 1. $Q_4 = 0$ indicates that a loop can be continuously deformed to the Γ point without closing the gap. This is because $Q_4 = 0$ when it is evaluated at the Γ point with a gapped spectrum, which follows from $\det D(\Gamma) = 1$ due to the Kramers degeneracy. Therefore, $Q_4 = 0$ corresponds to the trivial surface spectrum, whereas $Q_4 = 1$ indicates the surface anomaly. One can confirm this by noting that Q_4 captures the representation of the C_{4z} operator at the Γ point. Let us consider the case with $\delta H_{\Delta} = 0$, where all MFs merge at the Γ point. In this case, H_{BdG} has a block-diagonalized form, in which the 2×2 block with $\tau_z \pm 1$ has the form $H = -\mu \pm (k_x \sigma_x + k_y \sigma_y)$. As shown in Methods, for a two-band Hamiltonian $H = -\mu \pm (k_x \sigma_x + k_y \sigma_y)$, the representation $C_{4z} = (-1)^s e^{-i \frac{\pi}{2} \sigma_z}$ gives $Q_4 = s$. Accordingly, for the 4×4 Hamiltonian H_{BdG} , the representation $C_{4z} = \tau_z e^{-i \frac{\pi}{2} \sigma_z}$ gives $Q_4 = 0 + 1 = 1$. From our analysis of the mass term above, we see that $Q_4 = 1$ indeed indicates the global stability of QMF.

We note that a QMF realized by odd- C_4 pairing accompanies gapless Majorana hinge states between gapped side surfaces, as shown in Fig. 1. The appearance of hinge states

can be attributed to the d -wavelike symmetry of the pairing function in real space (See Methods).

Classification table. Table II summarizes our topological classification of rotation-protected Majorana surface states. There are four types of Majorana surface states indicated by $\mathbb{Z}_{U(1)}$, \mathbb{Z}_{HS} , $(\mathbb{Z}_2)_{DC}$, and $(\mathbb{Z}_2)_Q$, respectively. All these states can exist only when time reversal T symmetry is present because point nodes or contractible loops on the surface BZ cannot be protected by P and C_n symmetries only. Here, $\mathbb{Z}_{U(1)}$ stands for the total $U(1)$ winding number of Majorana fermions protected by chiral symmetry. This invariant is nontrivial only for even- C_n pairing, because otherwise C_n symmetry trivializes the total winding number. The winding number is also trivialized by time reversal symmetry when $T^2 = P^2$ (See Methods). The remaining three anomalous surface states characterized by \mathbb{Z}_{HS} , $(\mathbb{Z}_2)_{DC}$, $(\mathbb{Z}_2)_Q$ are new surface states protected by C_n symmetry, which correspond to HSMFs, DCMFLs, QMFs, respectively, on C_n -invariant surfaces. While HSMFs can appear with even- C_n pairing, DCMFL and QMF can appear with odd- $C_{2,6}$ and odd- C_4 pairings, respectively, in spin-orbit coupled systems (the first row in Table II). While we focus on the superconductivity in spin-orbit coupled systems, spin-SU(2)-symmetric systems, and spin-polarized systems in Table II, our approach can be applied to other symmetry classes as well. We provide an extended classification table in SM, which includes both linear and projective representation $C_n^n = \pm 1$ for AZ classes DIII, CI, CII, and BDI with the assumption of the commutation relation $C_n T = T C_n$.

Lattice model. To demonstrate our theory, we consider the following model Hamiltonian describing a doped \mathbb{Z}_2 TI or Dirac semimetal

$$h_1 = -\mu + f_1 \rho_z + f_2 \rho_x \sigma_z + f_3 \rho_y + f_4 \rho_x \sigma_x + f_5 \rho_x \sigma_y, \quad (9)$$

where $\rho_{i=x,y,z}$ and $\sigma_{i=x,y,z}$ are Pauli matrices for orbital and spin degrees of freedom, respectively, and $f_1 = 4 - 2(\cos k_x + \cos k_y) - \cos k_z$, $f_2 = \sin k_x$, $f_3 = -\sin k_y$, $f_4 = 3 \sin k_z (\cos k_y - \cos k_x) + m_0 \sin k_z$, and $f_5 = -\sin k_z \sin k_x \sin k_y + m_1 \sin k_z$. It is symmetric under time reversal $\mathcal{T} = i\sigma_y K$ and mirror operations $\mathcal{M}_x : (x, y, z) \rightarrow (-x, y, z)$, $\mathcal{M}_y : (x, y, z) \rightarrow (x, -y, z)$, $\mathcal{M}_z : (x, y, z) \rightarrow (x, y, -z)$, which are represented by $\mathcal{M}_x = i\sigma_x$, $\mathcal{M}_y = i\rho_z \sigma_y$, and $\mathcal{M}_z = i\sigma_z$, respectively. This model describes a C_{4z} symmetric Dirac semimetal when $m_0 = m_1 = 0$. Nonzero m_0 and m_1 , which breaks C_{4z} , M_x , and M_y symmetries, opens a gap at bulk Dirac points leading to a \mathbb{Z}_2 TI [63, 64].

We first consider even- C_{2z} pairing. When μ is small, since the $\mathbf{k} = (0, 0, k_z)$ line is the only C_2 -invariant line crossing the Fermi surface, we need a 1D TSC with $w_+ = -w_- = 2$ along the $\mathbf{k} = (0, 0, k_z)$ line to observe a HSMF. If we choose a pairing function $\Delta(\mathbf{k}) = \Delta_e \sin k_z \sigma_z$, the resulting BdG Hamiltonian along the $\mathbf{k} = (0, 0, k_z)$ line is $H_{\text{BdG}} = -\mu \tau_z - \cos k_z \rho_z \tau_z + \Delta_e \sin k_z \sigma_z \tau_x$, where $\tau_{i=x,y,z}$ are Pauli matrices for particle-hole indices, and $m_0 = m_1 = 0$ is as-

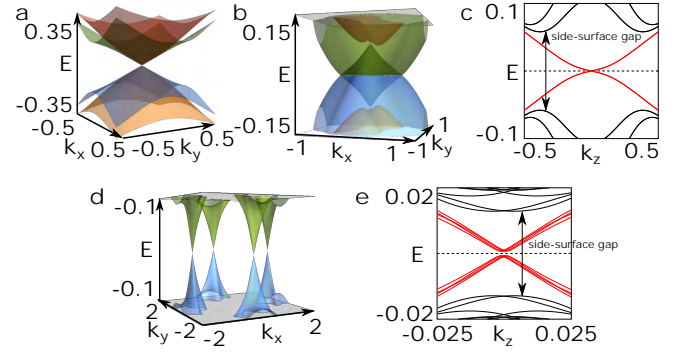


FIG. 5. Boundary Majorana surface states in lattice models. **a.** Spin-3/2 Majorana fermion obtained from Eq. (44) with $\mu = 0.5$, $m_0 = m_1 = 0$ and even- C_2 pairing $\Delta_e = 0.5$. **b.** A doubly charged Majorana Fermi line on a C_2 invariant surface obtained from Eq. (44) with $\mu = 0.5$, $m_0 = m_1 = 0.3$ and odd- C_2 pairing $\Delta_o = 0.3$. **c.** The helical hinge state (red color) for odd- C_2 pairing obtained from the same Hamiltonian used in **b.** **d.** A quartet of spin-1/2 Majorana fermions obtained from Eq. (46) with $\mu = 0.2$, $M = 1.5$, $\lambda_{\text{SO}} = 0.1$, and $\Delta_{x^2-y^2} = \Delta_{xy} = 0.5$. Associated hinge states (red color) are shown in **e.** In **e**, an additional pairing term $\delta\Delta = 0.1(\sin k_x \rho_x \sigma_y + \sin k_y \rho_y \sigma_x)$ is added to open the gap on the side surfaces. The splitting of the four C_{4z} -related hinge spectra and the small gap at zero energy are finite-size effects, which get reduced exponentially as the size of the system grows. The energy spectra in **a**, **b**, and **d** are calculated with 40 unit cells along the z direction and the periodic boundary condition along the x, y directions. **c** and **e** are calculated with 20×20 unit cells along the x and y directions and the periodic boundary condition along the z direction.

sumed for simplicity. Since H_{BdG} is diagonal in the spin and orbital indices, it can be labelled as $H_{\text{BdG}}^{s_\rho, s_\sigma}$ where s_ρ and s_σ indicate the eigenvalues of ρ_z and σ_z , respectively. Then, one can show that each 2×2 matrix $H_{\text{BdG}}^{s_\rho, s_\sigma}$ has the winding number $w_{s_\rho, s_\sigma} = -s_\rho s_\sigma$ for $S = \tau_y$, which gives $w_+ = -w_- = 2$ for $C_{2z} = -i\rho_z \sigma_z$. The associated surface spectrum with a spin-3/2 fermion at $(k_x, k_y) = (0, 0)$ on the C_{2z} -invariant surface is shown in Fig. 2(a). When other even- C_2 pairing terms dominate, a nodal superconductor or a topologically trivial superconductor can also be obtained [See SN].

On the other hand, in the case of odd- C_2 pairing, since the presence of a single Dirac fermion on the surface is the key ingredient for observing a DCMFL, any odd- C_2 pairing can induce a DCMFL, thus realizing a C_2 -protected TSC as long as the bulk gap fully opens. The surface spectrum for $\Delta(\mathbf{k}) = \Delta_o \rho_x$ is shown in Fig. 2(b). Here, we need both nonzero m_0 and m_1 to obtain a fully gapped TSC, because otherwise there appear Dirac points protected by either C_4 symmetry [63, 64] or mirror symmetry [65]. We note that even if the surface Dirac cone is buried in the bulk states, since the bulk states do not contribute to π -Berry phase, a DCMFL can still be observed. In addition to DCMFLs, we obtain helical Majorana hinge states on side surfaces as shown in Fig. 2(c).

To describe an odd- C_4 TSC with QMF, we need a model whose Fermi surface does not cross C_4 -invariant lines, because otherwise the bulk gap does not fully open for odd- C_4

pairing. Hence, instead of Eq. (44), we consider the following model Hamiltonian for a doped \mathbb{Z}_2 TI,

$$h_2 = -\mu + \sin k_z \rho_y + (M - \sum_{i=x,y,z} \cos k_i) \rho_z + \lambda_{\text{SO}} (\sin k_x \rho_x \sigma_y - \sin k_y \rho_y \sigma_x), \quad (10)$$

where $\rho_{i=x,y,z}$ ($\sigma_{i=x,y,z}$) are the Pauli matrices for orbital (spin) degrees of freedom, and λ_{SO} indicates spin-orbit coupling. h_2 is symmetric under $\mathcal{T} = i\sigma_y K$, $\mathcal{M}_x = i\sigma_x$, $\mathcal{M}_y = i\sigma_y$, $\mathcal{M}_z = i\rho_z \sigma_z$, and $\mathcal{C}_{4z} = e^{-i\frac{\pi}{4}\sigma_z}$. When $\lambda_{\text{SO}} = 0$, h_2 describes a spin-SU(2) symmetric nodal line semimetal with a nodal loop along $\sin^2 k_x + \sin^2 k_y = M - 1$ on the $k_z = 0$ plane when $1 < M < 3$. If we take $|\mu|$ larger than the gap induced by λ_{SO} , the system has a torus-shaped Fermi surface, which is a characteristic of nodal line semimetals. Since this Fermi surface does not cross a C_{4z} -invariant line, a fully gapped TSC can be obtained by introducing an odd- C_{4z} pairing. If we consider a d -wave pairing $\Delta_d(\mathbf{k}) = \Delta_{x^2-y^2}(\cos k_y - \cos k_x)\rho_y \sigma_z + \Delta_{xy} \sin k_x \sin k_y \rho_x$, the bulk gap fully opens, and a QMF appears on the surface. When other odd- C_4 pairing terms are considered, either a nodal superconductor or a topologically trivial superconductor can also be obtained. The surface spectrum for the d -wave pairing is shown in Fig. 2(d), where one can clearly observe a QMF on the C_{4z} invariant surface. However, our d -wave pairing does not open the gap on the side surfaces. This is because $\Delta_d(\mathbf{k})$, which is odd under C_{4z} , is also odd under M_z , so that there appear gapless Majorana surface states protected by M_z symmetry on the side surfaces. Therefore, to open the side surface gap and observe the hinge states, we add an additional odd- C_4 pairing term $\delta\Delta(\mathbf{k}) \propto \sin k_x \rho_x \sigma_y + \sin k_y \rho_y \sigma_x$ which is even under M_z . The corresponding energy spectrum of the in-gap hinge states is shown in Fig. 2(e).

Discussion

Let us consider the effect of additional inversion I symmetry. Although I symmetry is broken on each C_n -invariant surface, it affects the surface states by constraining the bulk topology of superconductors. When the pairing function is invariant under I (i.e., even-parity), it is hard to realize rotation-protected TSCs. In the case of even- C_n pairing, the even-parity condition forces each C_n eigensector to have a trivial winding number along the C_n -invariant line, and thus HSMFs cannot be realized. On the other hand, in the case of odd- C_2 pairing with even-parity, the superconducting state in weak pairing limit has point (line) nodes when the bulk Fermi surface crosses a C_2 -invariant line (IC_2 -invariant plane) in the normal state [66–68]. Only odd- C_4 pairing does not have such a constraint from the even-parity pairing.

In contrast, odd-parity pairing is compatible with rotation-protected TSCs for both even- and odd- C_n pairings, consistent with our model calculations in Fig. 2. According to previous studies [11, 38, 69], an odd-parity pairing in doped \mathbb{Z}_2 topological insulators leads to second-order TSCs with gapless Majorana fermions along hinges forming an odd number of closed loops on the boundary. In the presence of an additional C_n symmetry, the C_n -invariant surfaces should

be gapless because otherwise the global configuration of the hinge states cannot form an odd number of closed loops on the whole boundary. This predicts a DCMFL for odd- C_2 pairing, because it is the only possible stable surface state on the C_2 invariant surface. For even- C_n pairing, HSMF can appear when the total winding number becomes zero due to other symmetries. This analysis shows that HSMFs or DCMFLs are generally expected from odd-parity superconductivity in doped \mathbb{Z}_2 topological insulators with rotational symmetry. Similar surface states appear in the superconducting state of doped Dirac semimetals while the bulk superconducting gap does not open. We note that a DCMFL was observed in a model of iron-based superconductors, described by a Dirac semimetal with an odd-parity pairing, although its doubly charged nature was not recognized [37].

Summary

To sum up, we propose two different ways of generating anomalous Majorana boundary states. One is through the anomalous representation of crystalline symmetry, which mixes the particle and hole degrees of freedom. The other is through nodal structures carrying multiple topological charges. By carefully investigating the stability of gapless Majorana surface states, we obtain the classification table for the anomalous Majorana surface states of 3D TSCs protected by rotational symmetry shown in Table II, which is consistent with the related preceding works [20, 22, 58, 59]. We believe that our theory provides a useful guide for the complete classification of TCSCs and understanding their bulk-boundary correspondence.

Methods

Spin-rotation-symmetric BdG Hamiltonian. Let us investigate the effect of spin rotation symmetry on the BdG Hamiltonian following Ref. [62]. When a system has a spin-rotational symmetry around the z axis, it is more effective to use the BdG Hamiltonian defined for each spin- z eigensector separately. If we assume a single pairing, the BdG Hamiltonian for the spin up sector has the following form

$$H_{\text{BdG}}^{\uparrow\uparrow}(\mathbf{k}) = \begin{pmatrix} h_{\uparrow\uparrow}(\mathbf{k}) & \Delta_{\uparrow\downarrow}(\mathbf{k}) \\ (\Delta_{\uparrow\downarrow}(\mathbf{k}))^\dagger & -(\tilde{U}_T)^t h_{\downarrow\downarrow}^t(-\mathbf{k}) \tilde{U}_T^* \end{pmatrix}, \quad (11)$$

where we use that $U_T = i\sigma_y \otimes \tilde{U}_T$. Here, the corresponding Nambu spinor is $\hat{\Psi}_\uparrow = (\hat{c}_{\uparrow\mathbf{k}}, \hat{c}_{\downarrow,-\mathbf{k}}^\dagger \tilde{U}_T^t)^t$. The spin-up BdG Hamiltonian belongs to the class A because there is no nonspatial symmetry constraint. If time reversal symmetry is present, the symmetry constraint $\tilde{U}_T [H_{\text{BdG}}^{\uparrow\downarrow}(\mathbf{k})]^* \tilde{U}_T^{-1} = H_{\text{BdG}}^{\uparrow\uparrow}(-\mathbf{k})$ is identical to the chiral symmetry

$$\tau_y H_{\text{BdG}}^{\uparrow\uparrow}(\mathbf{k}) \tau_y^{-1} = -H_{\text{BdG}}^{\uparrow\uparrow}(\mathbf{k}), \quad (12)$$

where τ_y is a Pauli matrix for the particle-hole indices. Therefore, a spin- z -preserving superconductor with time reversal symmetry belongs to the AZ symmetry class AIII.

Let us now consider the full spin SU(2) rotation symmetry. Since spin SU(2) rotation symmetry imposes that $h_{\uparrow\uparrow}(\mathbf{k}) =$

$h_{\downarrow\downarrow}(\mathbf{k})$, we can define the spinless BdG Hamiltonian as

$$\tilde{H}_{\text{BdG}}(\mathbf{k}) \equiv H_{\text{BdG}}^{\uparrow\uparrow}(\mathbf{k}) = \begin{pmatrix} \tilde{h}(\mathbf{k}) & \tilde{\Delta}(\mathbf{k}) \\ \tilde{\Delta}^\dagger(\mathbf{k}) & -(\tilde{U}_T)^t \tilde{h}^t(-\mathbf{k}) \tilde{U}_T^* \end{pmatrix}, \quad (13)$$

where we define $\tilde{h}(\mathbf{k}) \equiv h_{\uparrow\uparrow}(\mathbf{k}) = h_{\downarrow\downarrow}(\mathbf{k})$ and $\tilde{\Delta}(\mathbf{k}) \equiv \Delta_{\uparrow\downarrow}(\mathbf{k})$. Here, compared to the case without spin rotation symmetry, we have a reversed sign for the condition that the pairing function satisfy: $\tilde{\Delta}(\mathbf{k}) = +\tilde{U}_T^\dagger \tilde{\Delta}^t(-\mathbf{k}) \tilde{U}_T^*$. Accordingly, the particle-hole operator for the spinless BdG Hamiltonian takes the form

$$\tilde{P} = \begin{pmatrix} 0 & \tilde{U}_T \\ -(\tilde{U}_T)^t & 0 \end{pmatrix} K, \quad (14)$$

which satisfy $\tilde{P}^2 = -1$. Thus, a spin-SU(2)-symmetric BdG Hamiltonian is in the class C. When time reversal symmetry is present, the combination of time reversal and a spin π -rotation defines effective spinless time reversal symmetry satisfying $\tilde{T}^2 = +1$, so the BdG Hamiltonian belongs to the class CI.

Up to now, we assume spin-singlet pairing. In spin-polarized normal metals, however, triplet pairing should occur, so the relevant BdG Hamiltonian takes the form

$$H_{\text{BdG}}^{\uparrow\uparrow}(\mathbf{k}) = \begin{pmatrix} h_{\uparrow\uparrow}(\mathbf{k}) & \Delta_{\uparrow\uparrow}(\mathbf{k}) \\ (\Delta_{\uparrow\uparrow}(\mathbf{k}))^\dagger & -(\tilde{U}_T)^t h_{\uparrow\uparrow}^t(-\mathbf{k}) \tilde{U}_T^* \end{pmatrix}, \quad (15)$$

where we suppose that spins are polarized along the \uparrow direction. It has particle-hole symmetry under

$$\tilde{P} = \begin{pmatrix} 0 & \tilde{U}_T \\ (\tilde{U}_T)^t & 0 \end{pmatrix} K, \quad (16)$$

where $\tilde{P}^2 = 1$. While the spin polarization breaks time reversal symmetry and spin rotation symmetry individually, there remains a symmetry under the combination of time reversal and a spin rotation around the axis perpendicular to the spin-ordering axis. Since this effective time reversal \tilde{T} satisfies $\tilde{T}^2 = +1$, the BdG Hamiltonian belongs to the class BDI.

Berry phase on time-reversal-invariant loops. Here we show that the Berry phase on a time-reversal-invariant loops is always trivial in spinless systems with time reversal symmetry.

Before we study the Berry phase around a time-reversal-invariant loop, let us first summarize the definition and some useful properties of the abelian Berry connection $A(\mathbf{k})$ for the occupied states (i.e., $E < 0$ states in the Bogoliubov-de Gennes formalism). The abelian Berry connection is defined by

$$A(\mathbf{k}) = \sum_{n \in \text{occ}} \langle u_{n\mathbf{k}} | i \nabla_{\mathbf{k}} | u_{n\mathbf{k}} \rangle. \quad (17)$$

When the matrix element of time reversal operator at \mathbf{k} is given by

$$B_{mn}(\mathbf{k}) = \langle u_{m-\mathbf{k}} | T | u_{n\mathbf{k}} \rangle, \quad (18)$$

which satisfies

$$B(-\mathbf{k}) = (-1)^{s_T} B^t(\mathbf{k}) \quad (19)$$

when $T^2 = (-1)^{s_T} = \pm 1$, the Berry connection satisfies the following constraint

$$A(\mathbf{k}) = A(-\mathbf{k}) - i \nabla_{\mathbf{k}} \log \det B(\mathbf{k}). \quad (20)$$

Now we suppose that the band gap is open on a time-reversal-invariant loop $l = l_0 + T l_0$, where l_0 is an arc whose starting- and end-points are nonzero \mathbf{k}_0 and $-\mathbf{k}_0$. Then, the Berry phase Φ_l on the loop l is

$$\begin{aligned} \Phi_l &= \oint_l d\mathbf{k} \cdot A(\mathbf{k}) \\ &= \int_{l_0} d\mathbf{k} \cdot A(\mathbf{k}) + \int_{T l_0} d\mathbf{k} \cdot A(\mathbf{k}) \\ &= \int_{l_0} d\mathbf{k} \cdot [A(-\mathbf{k}) - i \nabla_{\mathbf{k}} \log \det B(\mathbf{k})] + \int_{T l_0} d\mathbf{k} \cdot A(\mathbf{k}) \\ &= -i \int_{\mathbf{k}_0}^{-\mathbf{k}_0} d\mathbf{k} \cdot \nabla_{\mathbf{k}} \log \det B(\mathbf{k}) \\ &= -i \log \left[\frac{\det B(-\mathbf{k}_0)}{\det B(\mathbf{k}_0)} \right] \\ &= -i \log [(-1)^{N_{\text{occ}} s_T}] \\ &= \pi N_{\text{occ}} s_T \pmod{2\pi}, \end{aligned} \quad (21)$$

where we use in the fourth line that $\oint_{l_0} d\mathbf{k} \cdot A(-\mathbf{k}) = -\oint_{T l_0} d(T\mathbf{k}) \cdot A(T\mathbf{k}) = -\oint_{T l_0} d\mathbf{k} \cdot A(\mathbf{k})$, N_{occ} is the number of the occupied states on the loop and use Eq. (19) in the sixth line.

Our derivation shows that in spinless systems where $T^2 = 1$, the Berry phase around a time-reversal-invariant loop is always zero (mod 2π). Thus, band crossing carrying Berry phase π (in particular, a 2D Dirac point) cannot appear at a time-reversal-invariant momentum (TRIM) in spinless systems.

Alternatively, the same conclusion can be drawn for a 2D Dirac point by investigating the Hamiltonian. We consider the most general form of an effective two-level Hamiltonian around a TRIM ($\mathbf{k} = 0$).

$$H(\mathbf{k}) = \mu(\mathbf{k}) + f_1(\mathbf{k})\sigma_x + f_2(\mathbf{k})\sigma_y + f_3(\mathbf{k})\sigma_z. \quad (22)$$

If we take a basis where $T = K$ without loss of generality, we find

$$\begin{aligned} \mu(k_x, k_y) &= \mu(-k_x, -k_y) \\ f_{1,3}(k_x, k_y) &= f_{1,3}(-k_x, -k_y) \\ f_2(k_x, k_y) &= -f_2(-k_x, -k_y). \end{aligned} \quad (23)$$

Since only f_2 is an odd function of \mathbf{k} , while a Dirac point at a TRIM requires two independent components of $\mathbf{f} = (f_1, f_2, f_3)$ to be odd in \mathbf{k} , we cannot achieve a Dirac point even after considering any other symmetry.

Symmetry of the winding number. Here, we study the symmetry properties of the 1D and 3D winding numbers under

crystalline and time reversal symmetries.

Let G be a point group symmetry operator. Then, the 3D winding number in G -symmetric systems satisfies

$$\begin{aligned}
 w_{3D} &= \frac{1}{48\pi^2} \int_{\text{BZ}} d^3k \epsilon^{ijk} \text{Tr} [S H^{-1} \partial_{k_i} H H^{-1} \partial_{k_j} H H^{-1} \partial_{k_k} H] \\
 &= \frac{1}{48\pi^2} \int_{\text{BZ}} d^3k \epsilon^{ijk} \text{Tr} [(G S G^{-1}) H^{-1} (G \mathbf{k}) \partial_{k_i} H (G \mathbf{k}) H^{-1} (G \mathbf{k}) \partial_{k_j} H (G \mathbf{k}) H^{-1} (G \mathbf{k}) \partial_{k_k} H (G \mathbf{k})] \\
 &= \frac{1}{48\pi^2} \int_{\text{BZ}} d^3k \epsilon^{ijk} (\det G) \text{Tr} [(G S G^{-1}) H^{-1} \partial_{k_i} H H^{-1} \partial_{k_j} H H^{-1} \partial_{k_k} H]_{G \mathbf{k}} \\
 &= \frac{(\det G)}{48\pi^2} \int_{\text{BZ}} d^3k \epsilon^{ijk} \text{Tr} [(G S G^{-1}) H^{-1} \partial_{k_i} H H^{-1} \partial_{k_j} H H^{-1} \partial_{k_k} H] \\
 &= \pm (\det G) w_{3D}.
 \end{aligned} \tag{24}$$

where we used that the Hamiltonian H is G -symmetric, and the sign in the last line indicates the G -parity of the pairing function $U_G \Delta(\mathbf{k}) U_G^{-1} = \Delta(R_G \mathbf{k})$, where $R_G \mathbf{k}$ is the natural transformation of \mathbf{k} under G . It shows that $w_{3D} = 0$ for odd- C_n pairing, even- M , or even- I pairing.

This is consistent with the constraint on the sum of winding numbers carried by MFs on G -invariant surfaces for $G = C_n$ or M . Let l be a G -invariant (invariant up to orientation reversal) loop in a 2D Brillouin zone. The winding number w_l around the loop then satisfies

$$\begin{aligned}
 w_l &= \frac{i}{4\pi} \oint_l d\mathbf{k} \cdot \text{Tr} [S H^{-1} \nabla_{\mathbf{k}} H] \\
 &= \frac{i}{4\pi} \oint_l d\mathbf{k} \cdot \text{Tr} [S G^{-1} H^{-1} (G \mathbf{k}) G \nabla_{\mathbf{k}} G^{-1} H (G \mathbf{k}) G] \\
 &= \frac{i}{4\pi} \oint_l d\mathbf{k} \cdot \text{Tr} [(G S G^{-1}) H^{-1} (G \mathbf{k}) \nabla_{\mathbf{k}} H (G \mathbf{k})] \\
 &= \frac{i}{4\pi} \oint_{G \cdot l} d(G \mathbf{k}) \cdot \text{Tr} [(G S G^{-1}) H^{-1} (G \mathbf{k}) \nabla_{G \mathbf{k}} H (G \mathbf{k})] \\
 &= \frac{i}{4\pi} (\det G) \oint_l d\mathbf{k} \cdot \text{Tr} [(G S G^{-1}) H^{-1} \nabla_{\mathbf{k}} H] \\
 &= \pm (\det G) w_l,
 \end{aligned} \tag{25}$$

where we use that $\oint_{G \cdot l} = (\det G) \oint_l$ in the fifth line. Since $w_l = 0$ for any G -invariant loop in the case of odd- C_n or even- M pairing, the total winding number in the surface Brillouin zone should be zero.

Let us also consider the 1D winding number w_{1D} defined on a noncontractible loop, which is a 1D Brillouin zone.

$$w_{1D} = \frac{i}{4\pi} \int_{1D \text{ BZ}} dk \text{Tr} [S H^{-1} \nabla_k H]. \tag{26}$$

We have

$$w_{1D} = \pm s_G w_{1D}, \tag{27}$$

where the sign in front of s_G captures the G -parity of the pairing function, and $s_G = \pm 1$ is defined by $Gk = s_G k$.

Similarly, one can show that for time reversal symmetry,

$$\begin{aligned}
w_{3D} &= \frac{1}{48\pi^2} \int_{\text{BZ}} d^3k \epsilon^{ijk} \text{Tr} [S H^{-1} \partial_{k_i} H H^{-1} \partial_{k_j} H H^{-1} \partial_{k_k} H] \\
&= \frac{1}{48\pi^2} \int_{\text{BZ}} d^3k \epsilon^{ijk} \text{Tr} [S T^{-1} H^{-1}(-\mathbf{k}) \partial_{k_i} H(-\mathbf{k}) H^{-1}(-\mathbf{k}) \partial_{k_j} H(-\mathbf{k}) H^{-1}(-\mathbf{k}) \partial_{k_k} H(-\mathbf{k}) T] \\
&= -\frac{1}{48\pi^2} \int_{\text{BZ}} d^3k \epsilon^{ijk} \text{Tr} [(U_T^* S (U_T^*)^{-1}) (H^{-1} \partial_{k_i} H H^{-1} \partial_{k_j} H H^{-1} \partial_{k_k} H)^*]_{-\mathbf{k}} \\
&= \left\{ -\frac{1}{48\pi^2} \int_{\text{BZ}} d^3k \epsilon^{ijk} \text{Tr} [(U_T S^* U_T^{-1}) H^{-1} \partial_{k_i} H H^{-1} \partial_{k_j} H H^{-1} \partial_{k_k} H]_{-\mathbf{k}} \right\}^* \\
&= \left\{ -\frac{1}{48\pi^2} \int_{\text{BZ}} d^3k \epsilon^{ijk} \text{Tr} [(T^{-1} S T) H^{-1} \partial_{k_i} H H^{-1} \partial_{k_j} H H^{-1} \partial_{k_k} H]_{-\mathbf{k}} \right\}^* \\
&= -\frac{1}{48\pi^2} \int_{\text{BZ}} d^3k \epsilon^{ijk} \text{Tr} [(T^{-1} S T) H^{-1} \partial_{k_i} H H^{-1} \partial_{k_j} H H^{-1} \partial_{k_k} H].
\end{aligned} \tag{28}$$

Note that the requirement $S^2 = 1$ needed for the above expression of the winding number is satisfied when we define S as

$$S = i^{s_T + s_C} T C, \tag{29}$$

with the convention $T C = C T$, where $T^2 = (-1)^{s_T}$ and $C^2 = (-1)^{s_C}$. Therefore,

$$T^{-1} S T = (-1)^{s_T + s_C} S. \tag{30}$$

Thus, we have

$$w_{3D} = -(-1)^{s_T + s_C} w_{3D}. \tag{31}$$

This shows that the winding number is trivial in the classes BDI and CII where $(-1)^{s_T + s_C} = +1$. One can also derive

$$w_l = -(-1)^{s_T + s_C} w_l. \tag{32}$$

In contrast, we have

$$w_{1D} = +(-1)^{s_T + s_C} w_{1D}, \tag{33}$$

such that the winding number in the 1D Brillouin zone is trivial in the classes DIII and CI. More generally, if we consider a C_n -invariant line, the winding number w_{1D}^λ for each eigensector of C_n rotational symmetry with eigenvalue λ satisfies

$$w_{1D}^\lambda = +(-1)^{s_T + s_C} w_{1D}^{\lambda*}. \tag{34}$$

Majorana Kramers pairs in spin-orbit coupled 2D systems. Here, we show the emergence of Majorana Kramers pairs on the boundary of superconductors obtained by odd- $C_{n=2,4,6}$ pairing in doped 2D \mathbb{Z}_2 topological insulators. To investigate the boundary states, let us begin with a low-energy effective Hamiltonian of the \mathbb{Z}_2 topological insulator.

$$h(\mathbf{k}) = -\mu + M\rho_z + k_x\rho_x\sigma_z + k_y\rho_y, \tag{35}$$

where $\rho_{i=x,y,z}$ and $\sigma_{i=x,y,z}$ are the Pauli matrices for the orbital and spin degrees of freedom. It is symmetric under

$$\mathcal{T} = i\sigma_y K, \quad C_n = e^{-i\frac{\pi}{n}\rho_z\sigma_z}. \tag{36}$$

The corresponding Bogoliubov-de Gennes (BdG) Hamiltonian has the form of the doubled \mathbb{Z}_2 topological superconductor.

$$\begin{aligned}
H_{\text{BdG}}(\mathbf{k}) &= M\tau_z\rho_z + k_x\tau_z\rho_x\sigma_z + k_y\tau_z\rho_y \\
&= M\Gamma_1 + k_x\Gamma_2 + k_y\Gamma_3,
\end{aligned} \tag{37}$$

where $\tau_{i=0,x,y,z}$ are Pauli matrices for the Nambu space, and we introduce 8×8 mutually anticommuting Gamma matrices

$$\begin{aligned}
\Gamma_1 &= \tau_z\rho_z & (+, -, +, +), \\
\Gamma_2 &= \tau_z\rho_x\sigma_z & (-, +, -, -), \\
\Gamma_3 &= \tau_z\rho_y & (-, +, -, -), \\
\Gamma_4 &= \tau_z\rho_x\sigma_x & (-, +, -, -), \\
\Gamma_5 &= \tau_z\rho_x\sigma_y & (-, +, -, -), \\
\Gamma_6 &= \tau_x & (+, -, +, -), \\
\Gamma_7 &= \tau_y & (+, +, +, -),
\end{aligned} \tag{38}$$

where the four signs show their commutation (+) or anticommutation (-) relations with

$$\begin{aligned}
T &= i\sigma_y K, \\
C &= \tau_y\sigma_y K, \\
C_{2z}^{\text{even}} &= -i\rho_z\sigma_z, \\
C_{2z}^{\text{odd}} &= -i\tau_z\rho_z\sigma_z,
\end{aligned} \tag{39}$$

in order. One can see that a superconducting gap $\Delta\Gamma_6$ is allowed for even- C_2 pairing, which shows that the bulk topology is trivial. However, C_4 symmetry forbids the bulk mass term because $C_{4z}^{\text{odd}} = \tau_z e^{-i\frac{\pi}{n}\rho_z\sigma_z}$ anticommutes with it. Therefore, the mass term is prohibited in the translation-invariant bulk for any odd- $C_{n=2,4,6}$ pairing. However, $\Delta\Gamma_6$ can describe the pairing gap on the boundary. We can see

this by allowing the position dependence of the pairing in real space [24, 25].

$$H(\mathbf{k}, \mathbf{r}) = M(\mathbf{r})\Gamma_1 + k_x\Gamma_2 + k_y\Gamma_3 + \Delta(\mathbf{r})\Gamma_6. \quad (40)$$

Here, $M(\mathbf{r})$ is the bulk mass term which approaches to a constant value deep in the bulk and to zero on the boundary, and $\Delta(\mathbf{r})$ is the surface pairing function that is nonzero only near the boundary, where translation symmetries are broken. Since $\Delta(R_n\mathbf{r}) = -\Delta(\mathbf{r})$ for odd- C_n pairing, the pairing gap has to close at $n \pmod{2n}$ points on the boundary. These are the locations where Majorana zero modes appear (often called Majorana corner modes [24, 25] because they usually appear at corners of the system [70]). The zero modes form a Kramers pair at each site because of time reversal symmetry. This shows that odd- C_n pairing on the helical edge states of a \mathbb{Z}_2 topological insulator induces Majorana Kramers pairs on the boundary.

Topological charges of a quartet of MFs for odd- C_4 pairing. Here we explain the topological invariant protecting the quartet of Majorana fermions. While such a configuration appears in C_4 -symmetric systems in ordinary superconductors, a similar configuration with two and six surface nodal points can appear in C_2 - and C_6 -symmetric topological crystalline insulators or spin-orbit coupled C_2 - and C_6 -symmetric superconductors with exotic particle-hole symmetry where $P^2 = -1$ [See SN]. With this in mind, we consider general $C_{n=2,4,6}$ -symmetric systems. Since particle-hole symmetry does not play an important role here, the results here can be applied to the surface states of topological crystalline insulators also.

Before we study the topological invariant around a C_n -invariant loop, let us first see how C_n symmetry constrains the abelian Berry connection $A(\mathbf{k})$ for the occupied states. When the matrix element of C_n operator is given by

$$D_{mn}(\mathbf{k}) = \langle u_{mR_n\mathbf{k}} | C_n | u_{n\mathbf{k}} \rangle, \quad (41)$$

the Berry connection satisfies the following constraint

$$A(\mathbf{k}) = R_n^{-1} \cdot A(R_n\mathbf{k}) + i\nabla_{\mathbf{k}} \log \det D(\mathbf{k}). \quad (42)$$

In spin-orbit coupled systems with both $C_{n=2,4,6}$ and time reversal symmetries, we can define a \mathbb{Z}_2 topological invariant Q_n over a $1/n$ segment of a C_n -invariant loop. We consider the Berry phase around a closed loop connecting $\Gamma = (0, 0)$, \mathbf{k}_0 , and $R_n\mathbf{k}_0$ for a nonzero \mathbf{k}_0 .

$$\begin{aligned} \Phi_{1/n}^{\mathbf{k}_0} &= \int_{\Gamma}^{\mathbf{k}_0} d\mathbf{k} \cdot \mathbf{A}(\mathbf{k}) + \int_{\mathbf{k}_0}^{R_n\mathbf{k}_0} d\mathbf{k} \cdot \mathbf{A}(\mathbf{k}) + \int_{R_n\mathbf{k}_0}^{\Gamma} d\mathbf{k} \cdot \mathbf{A}(\mathbf{k}) \\ &= \int_{\Gamma}^{\mathbf{k}_0} d\mathbf{k} \cdot \mathbf{A}(\mathbf{k}) + \int_{\mathbf{k}_0}^{R_n\mathbf{k}_0} d\mathbf{k} \cdot \mathbf{A}(\mathbf{k}) + \int_{\mathbf{k}_0}^{\Gamma} d\mathbf{k} \cdot R_n^{-1} \mathbf{A}(R_n\mathbf{k}) \\ &= \int_{\Gamma}^{\mathbf{k}_0} d\mathbf{k} i\nabla_{\mathbf{k}} \log \det D(\mathbf{k}) + \int_{\mathbf{k}_0}^{R_n\mathbf{k}_0} d\mathbf{k} \cdot \mathbf{A}(\mathbf{k}) \\ &= \pi Q_n^{\mathbf{k}_0} - i\nabla_{\mathbf{k}} \log \det D(\Gamma), \end{aligned} \quad (43)$$

where we define $Q_n^{\mathbf{k}_0}$ on a line connecting \mathbf{k}_0 and $R_n\mathbf{k}_0$:

$$Q_n^{\mathbf{k}_0} = \frac{i}{\pi} \log \det D(\mathbf{k}_0) + \frac{1}{\pi} \int_{\mathbf{k}_0}^{R_n\mathbf{k}_0} d\mathbf{k} \cdot \mathbf{A}(\mathbf{k}). \quad (44)$$

This quantity does not depend on the choice of the initial point \mathbf{k}_0 : $Q_{\mathbf{k}_0'} - Q_n^{\mathbf{k}_0} = 0$ on a given loop. Let us thus omit the subscript \mathbf{k}_0 for $Q_n^{\mathbf{k}_0}$. Also, Q_n is gauge invariant under $|u_{n\mathbf{k}}\rangle \rightarrow U_{mn} |u_{m\mathbf{k}}\rangle$, which transforms D and A by $D(\mathbf{k}) \rightarrow U^{-1}(R_n\mathbf{k})D(\mathbf{k})U(\mathbf{k})$ and $A(\mathbf{k}) \rightarrow A(\mathbf{k}) + i\nabla_{\mathbf{k}} \log \det U(\mathbf{k})$.

We can see that Q_n is quantized in the presence of time reversal symmetry by taking a real gauge where $C_2T |u_{n\mathbf{k}}\rangle = |u_{n\mathbf{k}}\rangle$. In a real gauge, $A(\mathbf{k}) = 0$ and $D(\mathbf{k})$ belongs to an orthogonal group such that $\det D = \pm 1$. From this, it follows that $Q_n = \pm 1$ in a real gauge. Moreover, since Q_n is gauge invariant,

$$Q_n = \pm 1 \quad (45)$$

holds in any gauge.

As is clear from the definition, Q_n is closely related to $\Phi_{1/n}^{\mathbf{k}_0}$, and they are equivalent for the purpose of studying the local stability of gapless points within the $1/n$ sector of the Brillouin zone. In fact, they are identical when the spectrum is gapped at Γ because $\det D(\Gamma) = 1$ due to Kramers degeneracy. However, when we study the global stability of gapless surface states protected by C_n symmetry, we need to use the invariant Q_n rather than the quantized Berry phase $\Phi_{1/n}^{\mathbf{k}_0}$. It is because $\Phi_{1/n}^{\mathbf{k}_0}$ cannot be defined in the case where all the gap closing points gather at the Γ point. To see whether such a critical gapless point at Γ can be gapped or not, we have to look at Q_n , which is well-defined on a fully gapped loop surrounding Γ .

This \mathbb{Z}_2 invariant Q_n is the topological invariant carried by the gapless surface states of $C_{n=2,4,6}$ -protected topological insulators proposed by Fang and Fu [19], while the authors did not figure out this topological invariant and relied on the low-energy effective Hamiltonian to study the protection of the gapless states. Let us take the real gauge such that $Q_n = (i/\pi) \log \det D(\mathbf{k}_0)$. If we contract the loop where Q_n is defined to a TRIM \mathbf{k}_{TRIM} , we always have $Q_n = 0$ in lattice systems because of the Kramers degeneracy, imposing $\det D(\mathbf{k}_{\text{TRIM}}) = 1$. Thus, $Q_n = 1$ reveals the rotation anomaly on the surface of topological crystalline insulators or superconductors. We remark that, while gapped spin-orbit coupled lattice systems always have $Q_n = 0$ because $\det D = 1$ by time reversal symmetry, Q_n can change by a band inversion in spinless systems. So, there is no surface anomaly due to nontrivial Q_n in spinless systems.

Our invariant Q_n is equivalent to the Wilson line invariant defined to capture fragile topology in C_6 -symmetric systems in Ref. [71, 72]. Let us define the Wilson line operator for the occupied states on the line connecting \mathbf{k}_2 and \mathbf{k}_1 by

$$W_{\mathbf{k}_2 \leftarrow \mathbf{k}_1} = \lim_{\delta \rightarrow 0} P_{\mathbf{k}_2} P_{\mathbf{k}' - \delta} \dots P_{\mathbf{k} + \delta} P_{\mathbf{k}_1}, \quad (46)$$

where

$$P_{\mathbf{k}} = \sum_{n \in \text{occ}} |u_{n\mathbf{k}}\rangle \langle u_{n\mathbf{k}}| \quad (47)$$

is the projection to the occupied states at momentum \mathbf{k} . Since the projection satisfies $P_{R_n\mathbf{k}} = C_n \sum_{n \in \text{occ}} |u_{n\mathbf{k}}\rangle \langle u_{n\mathbf{k}}| C_n^{-1}$ in C_n -symmetric systems, the Wilson line has the following property.

$$W_{R_n\mathbf{k}_2 \leftarrow R_n\mathbf{k}_1} = C_n W_{\mathbf{k}_2 \leftarrow \mathbf{k}_1} C_n^{-1} \quad (48)$$

Thus, the Wilson loop operator over a C_n -invariant loop with initial point \mathbf{k}_0 is given by

$$\begin{aligned} W_{\mathbf{k}_0 \leftarrow \mathbf{k}_0} &= W_{\mathbf{k}_0 \leftarrow C_n^{-1}\mathbf{k}_0} \cdots W_{R_n\mathbf{k}_0 \leftarrow \mathbf{k}_0} \\ &= C_n^{-1} W_{R_n\mathbf{k}_0 \leftarrow \mathbf{k}_0} C_n^{-(n-1)} \cdots W_{R_n\mathbf{k}_0 \leftarrow \mathbf{k}_0} \\ &= (-1)^{sT} (C_n^{-1} W_{R_n\mathbf{k}_0 \leftarrow \mathbf{k}_0})^n, \end{aligned} \quad (49)$$

where we use $C_n^{n-1} = (-1)^{sT} C_n^{-1}$. Then, if we define the C_n -Wilson line by

$$W_{mn}^{C_n} \equiv \langle u_{m\mathbf{k}_0} | C_n W_{R_n\mathbf{k}_0 \leftarrow \mathbf{k}_0} | u_{n\mathbf{k}_0} \rangle, \quad (50)$$

it is independent of \mathbf{k}_0 and gauge invariant up to similarity transformations, such that its spectrum is gauge invariant. This C_n -Wilson line is related to Q_n by

$$e^{iQ_n} = \det W^{C_n}. \quad (51)$$

Q_n can be exactly calculated analytically in the Dirac point limit. Let us first begin with a twofold degenerate Dirac point at the Γ point described by

$$h_m = k \begin{pmatrix} 0 & e^{-im\theta} \\ e^{im\theta} & 0 \end{pmatrix}. \quad (52)$$

At half filling, one state is occupied at nonzero \mathbf{k} , and it takes the form

$$|u_{\text{occ}}^m\rangle = \frac{1}{\sqrt{2}} \begin{pmatrix} 1 \\ -e^{im\theta} \end{pmatrix}. \quad (53)$$

h_m is symmetric under the n -fold rotation

$$C_n^{s,m} = (-1)^s \exp\left(-i \frac{m\pi}{n} \sigma_z\right). \quad (54)$$

Namely, $C_n^{s,m} h_m(k, \theta) (C_n^{s,m})^{-1} = h_m(k, \theta + \pi/n)$. The matrix element of the rotation operator is given by

$$D_n^{s,m}(\mathbf{k}_0) = \langle u_{R_n\mathbf{k}}^m | C_n^{s,m} | u_{\mathbf{k}}^m \rangle = (-1)^s e^{-\pi i m/n}. \quad (55)$$

Thus,

$$\frac{i}{\pi} \log \det D_n^{s,m}(\mathbf{k}_0) = -s + \frac{m}{n}. \quad (56)$$

On the other hand, the Berry connection is given by

$$\begin{aligned} A_\theta(\mathbf{k}) &= \langle u_{\text{occ}}^\pm | i\partial_\theta | u_{\text{occ}}^\pm \rangle = -\frac{m}{2}, \\ A_k(\mathbf{k}) &= \langle u_{\text{occ}}^\pm | i\partial_k | u_{\text{occ}}^\pm \rangle = 0, \end{aligned} \quad (57)$$

such that

$$\frac{1}{\pi} \int_{\mathbf{k}_0}^{R_n\mathbf{k}_0} d\mathbf{k} \cdot A(\mathbf{k}) = -\frac{m}{n}. \quad (58)$$

We have

$$Q_n = s \pmod{2}. \quad (59)$$

Thus, in the case of fourfold Dirac point formed by two identical twofold Dirac points,

$$h_{4 \times 4} = h_m \oplus h_l, \quad (60)$$

the rotation-protected topological charge is given by

$$Q_n = s + s' \pmod{2}, \quad (61)$$

where s and s' are defined for the rotation operator acting on h_m and h_l , respectively. It is consistent with the analysis based on the low-energy effective Hamiltonian in Ref. [19].

-
- [1] M. Z. Hasan and C. L. Kane, Colloquium: Topological insulators, *Rev. Mod. Phys.* **82**, 3045 (2010).
 - [2] H. B. Nielsen and M. Ninomiya, *No-go theorem for regularizing chiral fermions*, Tech. Rep. (Science Research Council, 1981).
 - [3] E. Witten, Three lectures on topological phases of matter, *La Rivista del Nuovo Cimento* **39**, 313 (2016).
 - [4] L. Fu, C. L. Kane, and E. J. Mele, Topological insulators in three dimensions, *Phys. Rev. Lett.* **98**, 106803 (2007).
 - [5] L. Fu, Topological crystalline insulators, *Phys. Rev. Lett.* **106**, 106802 (2011).

- [6] J. C. Y. Teo, L. Fu, and C. L. Kane, Surface states and topological invariants in three-dimensional topological insulators: Application to $\text{Bi}_{1-x}\text{Sb}_x$, *Phys. Rev. B* **78**, 045426 (2008).
- [7] T. H. Hsieh, H. Lin, J. Liu, W. Duan, A. Bansil, and L. Fu, Topological crystalline insulators in the SnTe material class, *Nat. Commun.* **3**, 1 (2012).
- [8] Z. Wang, A. Alexandradinata, R. J. Cava, and B. A. Bernevig, Hourglass fermions, *Nature* **532**, 189 (2016).
- [9] B. J. Wieder, B. Bradlyn, Z. Wang, J. Cano, Y. Kim, H.-S. D. Kim, A. M. Rappe, C. L. Kane, and B. A. Bernevig, Wallpaper fermions and the nonsymmorphic Dirac insulator, *Science* **361**,

- 246 (2018).
- [10] J. Kruthoff, J. de Boer, J. van Wezel, C. L. Kane, and R.-J. Slager, Topological classification of crystalline insulators through band structure combinatorics, *Phys. Rev. X* **7**, 041069 (2017).
 - [11] H. C. Po, A. Vishwanath, and H. Watanabe, Symmetry-based indicators of band topology in the 230 space groups, *Nat. Commun.* **8**, 50 (2017).
 - [12] B. Bradlyn, L. Elcoro, J. Cano, M. Vergniory, Z. Wang, C. Felser, M. Aroyo, and B. A. Bernevig, Topological quantum chemistry, *Nature* **547**, 298 (2017).
 - [13] W. A. Benalcazar, B. A. Bernevig, and T. L. Hughes, Quantized electric multipole insulators, *Science* **357**, 61 (2017).
 - [14] W. A. Benalcazar, B. A. Bernevig, and T. L. Hughes, Electric multipole moments, topological multipole moment pumping, and chiral hinge states in crystalline insulators, *Phys. Rev. B* **96**, 245115 (2017).
 - [15] Z. Song, Z. Fang, and C. Fang, $(d - 2)$ -dimensional edge states of rotation symmetry protected topological states, *Phys. Rev. Lett.* **119**, 246402 (2017).
 - [16] F. Schindler, A. M. Cook, M. G. Vergniory, Z. Wang, S. S. Parkin, B. A. Bernevig, and T. Neupert, Higher-order topological insulators, *Sci. Adv.* **4**, eaat0346 (2018).
 - [17] Z. Wang, B. J. Wieder, J. Li, B. Yan, and B. A. Bernevig, Higher-order topology, monopole nodal lines, and the origin of large fermi arcs in transition metal dichalcogenides XTe_2 ($X = Mo, W$), *Phys. Rev. Lett.* **123**, 186401 (2019).
 - [18] C. Fang and L. Fu, New classes of three-dimensional topological crystalline insulators: Nonsymmorphic and magnetic, *Phys. Rev. B* **91**, 161105(R) (2015).
 - [19] C. Fang and L. Fu, New classes of topological crystalline insulators having surface rotation anomaly, *Sci. Adv.* **5**, eaat2374 (2019).
 - [20] K. Shiozaki and M. Sato, Topology of crystalline insulators and superconductors, *Phys. Rev. B* **90**, 165114 (2014).
 - [21] K. Shiozaki, M. Sato, and K. Gomi, Topology of nonsymmorphic crystalline insulators and superconductors, *Phys. Rev. B* **93**, 195413 (2016).
 - [22] E. Cornfeld and A. Chapman, Classification of crystalline topological insulators and superconductors with point group symmetries, *Phys. Rev. B* **99**, 075105 (2019).
 - [23] J. Langbehn, Y. Peng, L. Trifunovic, F. von Oppen, and P. W. Brouwer, Reflection-symmetric second-order topological insulators and superconductors, *Phys. Rev. Lett.* **119**, 246401 (2017).
 - [24] E. Khalaf, Higher-order topological insulators and superconductors protected by inversion symmetry, *Phys. Rev. B* **97**, 205136 (2018).
 - [25] M. Geier, L. Trifunovic, M. Hoskam, and P. W. Brouwer, Second-order topological insulators and superconductors with an order-two crystalline symmetry, *Phys. Rev. B* **97**, 205135 (2018).
 - [26] L. Trifunovic and P. W. Brouwer, Higher-order bulk-boundary correspondence for topological crystalline phases, *Phys. Rev. X* **9**, 011012 (2019).
 - [27] F. Zhang, C. L. Kane, and E. J. Mele, Topological mirror superconductivity, *Phys. Rev. Lett.* **111**, 056403 (2013).
 - [28] Y. Ueno, A. Yamakage, Y. Tanaka, and M. Sato, Symmetry-protected Majorana fermions in topological crystalline superconductors: theory and application to Sr_2RuO_4 , *Phys. Rev. Lett.* **111**, 087002 (2013).
 - [29] Y. Tsutsumi, M. Ishikawa, T. Kawakami, T. Mizushima, M. Sato, M. Ichioka, and K. Machida, UPt_3 as a topological crystalline superconductor, *J. Phys. Soc.* **82**, 113707 (2013).
 - [30] W. A. Benalcazar, J. C. Y. Teo, and T. L. Hughes, Classification of two-dimensional topological crystalline superconductors and Majorana bound states at disclinations, *Phys. Rev. B* **89**, 224503 (2014).
 - [31] D. Varjas, F. de Juan, and Y.-M. Lu, Bulk invariants and topological response in insulators and superconductors with nonsymmorphic symmetries, *Phys. Rev. B* **92**, 195116 (2015).
 - [32] K. Shiozaki, M. Sato, and K. Gomi, Z_2 topology in nonsymmorphic crystalline insulators: Möbius twist in surface states, *Phys. Rev. B* **91**, 155120 (2015).
 - [33] Q.-Z. Wang and C.-X. Liu, Topological nonsymmorphic crystalline superconductors, *Phys. Rev. B* **93**, 020505 (2016).
 - [34] Y. Yanase and K. Shiozaki, Möbius topological superconductivity in UPt_3 , *Phys. Rev. B* **95**, 224514 (2017).
 - [35] A. Daido, T. Yoshida, and Y. Yanase, Z_4 topological superconductivity in $uCoGe$, *Phys. Rev. Lett.* **122**, 227001 (2019).
 - [36] N. Bultinck, B. A. Bernevig, and M. P. Zaletel, Three-dimensional superconductors with hybrid higher-order topology, *Phys. Rev. B* **99**, 125149 (2019).
 - [37] T. Kawakami and M. Sato, Topological crystalline superconductivity in dirac semimetal phase of iron-based superconductors, *Phys. Rev. B* **100**, 094520 (2019).
 - [38] S. Ono, Y. Yanase, and H. Watanabe, Symmetry indicators for topological superconductors, *Phys. Rev. Research* **1**, 013012 (2019).
 - [39] Z. Yan, Higher-order topological odd-parity superconductors, *Phys. Rev. Lett.* **123**, 177001 (2019).
 - [40] J. Ahn and B.-J. Yang, Higher-order topological superconductivity of spin-polarized fermions, *Phys. Rev. Research* **2**, 012060(R) (2020).
 - [41] S. Ono, H. C. Po, and H. Watanabe, Refined symmetry indicators for topological superconductors in all space groups, *Sci. Adv.* **6**, eaaz8367 (2020).
 - [42] M. Geier, P. W. Brouwer, and L. Trifunovic, Symmetry-based indicators for topological Bogoliubov-de Gennes Hamiltonians, Preprint at <http://arXiv.org/abs/1910.11271> (2019).
 - [43] K. Shiozaki, Variants of the symmetry-based indicator, Preprint at <http://arXiv.org/abs/1907.13632> (2019).
 - [44] A. Skurativska, T. Neupert, and M. H. Fischer, Atomic limit and inversion-symmetry indicators for topological superconductors, *Phys. Rev. Research* **2**, 013064 (2020).
 - [45] F. Schindler, B. Bradlyn, M. H. Fischer, and T. Neupert, Pairing obstructions in topological superconductors, Preprint at <http://arXiv.org/abs/2001.02682> (2020) (2020).
 - [46] Y. Lin and A. J. Leggett, Towards a particle-number conserving theory of Majorana zero modes in $p + ip$ superfluids, Preprint at <http://arXiv.org/abs/1803.08003> (2018).
 - [47] G. E. Volovik, *The Universe in a Helium Droplet*, Vol. 117 (Oxford Univ. Press, New York, 2009).
 - [48] P. Hosur, S. Ryu, and A. Vishwanath, Chiral topological insulators, superconductors, and other competing orders in three dimensions, *Phys. Rev. B* **81**, 045120 (2010).
 - [49] S. Ryu, A. P. Schnyder, A. Furusaki, and A. W. W. Ludwig, Topological insulators and superconductors: tenfold way and dimensional hierarchy, *New J. Phys.* **12**, 065010 (2010).
 - [50] M. P. Kennett, N. Komeilizadeh, K. Kaveh, and P. M. Smith, Birefringent breakup of dirac fermions on a square optical lattice, *Phys. Rev. A* **83**, 053636 (2011).
 - [51] B. Bradlyn, J. Cano, Z. Wang, M. Vergniory, C. Felser, R. J. Cava, and B. A. Bernevig, Beyond Dirac and Weyl fermions: Unconventional quasiparticles in conventional crystals, *Science* **353**, aaf5037 (2016).
 - [52] L. Liang and Y. Yu, Semimetal with both Rarita-Schwinger-Weyl and Weyl excitations, *Phys. Rev. B* **93**, 045113 (2016).

- [53] P. Tang, Q. Zhou, and S.-C. Zhang, Multiple types of topological fermions in transition metal silicides, *Phys. Rev. Lett.* **119**, 206402 (2017).
- [54] Y. Kim, B. J. Wieder, C. L. Kane, and A. M. Rappe, Dirac line nodes in inversion-symmetric crystals, *Phys. Rev. Lett.* **115**, 036806 (2015).
- [73] C. Fang, Y. Chen, H.-Y. Kee, and L. Fu, Topological nodal line semimetals with and without spin-orbital coupling, *Phys. Rev. B* **92**, 081201 (2015).
- [56] D. F. Agterberg, P. M. R. Brydon, and C. Timm, Bogoliubov Fermi surfaces in superconductors with broken time-reversal symmetry, *Phys. Rev. Lett.* **118**, 127001 (2017).
- [57] T. Bzdušek and M. Sigrist, Robust doubly charged nodal lines and nodal surfaces in centrosymmetric systems, *Phys. Rev. B* **96**, 155105 (2017).
- [58] K. Shiozaki, The classification of surface states of topological insulators and superconductors with magnetic point group symmetry, Preprint at <http://arXiv.org/abs/1907.09354> (2019).
- [59] C. Fang, B. A. Bernevig, and M. J. Gilbert, Topological crystalline superconductors with linearly and projectively represented C_n symmetry, Preprint at <http://arXiv.org/abs/1701.01944> (2017).
- [60] W. Su, J. Schrieffer, and A. J. Heeger, Solitons in polyacetylene, *Phys. Rev. Lett.* **42**, 1698 (1979).
- [61] C.-K. Chiu, J. C. Y. Teo, A. P. Schnyder, and S. Ryu, Classification of topological quantum matter with symmetries, *Rev. Mod. Phys.* **88**, 035005 (2016).
- [62] A. P. Schnyder, S. Ryu, A. Furusaki, and A. W. W. Ludwig, Classification of topological insulators and superconductors in three spatial dimensions, *Phys. Rev. B* **78**, 195125 (2008).
- [63] S. Kobayashi and M. Sato, Topological superconductivity in dirac semimetals, *Phys. Rev. Lett.* **115**, 187001 (2015).
- [64] T. Hashimoto, S. Kobayashi, Y. Tanaka, and M. Sato, Superconductivity in doped dirac semimetals, *Phys. Rev. B* **94**, 014510 (2016).
- [65] S. A. Yang, H. Pan, and F. Zhang, Dirac and weyl superconductors in three dimensions, *Phys. Rev. Lett.* **113**, 046401 (2014).
- [66] S. Kobayashi, S. Sumita, Y. Yanase, and M. Sato, Symmetry-protected line nodes and Majorana flat bands in nodal crystalline superconductors, *Phys. Rev. B* **97**, 180504 (2018).
- [67] S. Sumita and Y. Yanase, Unconventional superconducting gap structure protected by space group symmetry, *Phys. Rev. B* **97**, 134512 (2018).
- [68] S. Sumita, T. Nomoto, K. Shiozaki, and Y. Yanase, Classification of topological crystalline superconducting nodes on high-symmetry lines: Point nodes, line nodes, and Bogoliubov Fermi surfaces, *Phys. Rev. B* **99**, 134513 (2019).
- [69] E. Khalaf, H. C. Po, A. Vishwanath, and H. Watanabe, Symmetry indicators and anomalous surface states of topological crystalline insulators, *Phys. Rev. X* **8**, 031070 (2018).
- [70] Y. Hwang, J. Ahn, and B.-J. Yang, Fragile topology protected by inversion symmetry: Diagnosis, bulk-boundary correspondence, and wilson loop, *Phys. Rev. B* **100**, 205126 (2019).
- [71] B. Bradlyn, Z. Wang, J. Cano, and B. A. Bernevig, Disconnected elementary band representations, fragile topology, and wilson loops as topological indices: An example on the triangular lattice, *Phys. Rev. B* **99**, 045140 (2019).
- [72] A. Bouhon, A. M. Black-Schaffer, and R.-J. Slager, Wilson loop approach to fragile topology of split elementary band representations and topological crystalline insulators with time-reversal symmetry, *Phys. Rev. B* **100**, 195135 (2019).
- [73] C. Fang, Y. Chen, H.-Y. Kee, and L. Fu, Topological nodal line semimetals with and without spin-orbital coupling, *Phys. Rev. B* **92**, 081201 (2015).
- [74] J. Ahn, D. Kim, Y. Kim, and B.-J. Yang, Band topology and linking structure of nodal line semimetals with Z_2 monopole charges, *Phys. Rev. Lett.* **121**, 106403 (2018).

Acknowledgements

J.A. appreciates SangEun Han and James Jun He for helpful discussions. J.A. was supported by IBS-R009-D1. B.-J.Y. was supported by the Institute for Basic Science in Korea (Grant No. IBS-R009-D1) and Basic Science Research Program through the National Research Foundation of Korea (NRF) (Grant No. 0426-20200003). This work was supported in part by the U.S. Army Research Office under Grant Number W911NF-18-1-0137.

Supplementary Note for “Unconventional Majorana fermions on the surface of topological superconductors protected by rotational symmetry”

Junyeong Ahn^{1,2,3,4,5,*} and Bohm-Jung Yang^{1,2,3,†}

¹*Center for Correlated Electron Systems, Institute for Basic Science (IBS), Seoul 08826, Korea*

²*Department of Physics and Astronomy, Seoul National University, Seoul 08826, Korea*

³*Center for Theoretical Physics (CTP), Seoul National University, Seoul 08826, Korea*

⁴*RIKEN Center for Emergent Matter Science (CEMS), Wako, Saitama 351-0198, Japan*

⁵*Department of Applied Physics, The University of Tokyo, Bunkyo, Tokyo 113-8656, Japan*

CONTENTS

References	13
I. Classification of C_n -protected topological superconductors	2
A. Even- C_n (C_n -invariant) superconducting pairing	2
1. Chiral-symmetric systems without time reversal symmetry (class AIII)	2
2. Constraints from time reversal symmetry	3
3. AZ classes DIII and CI	3
4. AZ classes BDI and CII	4
5. Doubly charged Majorana Fermi lines	5
B. Odd- $C_{2,6}$ superconducting pairing	5
1. Doubly charged Majorana Fermi lines	5
2. Doublet and sextet of Majorana fermions	5
C. Odd- C_4 superconducting pairing	6
1. Doubly charged Majorana Fermi lines	6
2. Quartet of Majorana fermions	6
II. A model of spin-polarized C_2 -protected topological superconductor	7
III. Numerical calculation of topological charge of surface states in rotation-protected topological insulators	7
IV. Classification of pairing functions in Dirac semimetal and nodal line semimetal models	8

I. CLASSIFICATION OF C_n -PROTECTED TOPOLOGICAL SUPERCONDUCTORS

Let us classify topological superconductors protected by C_n symmetries. Before we move on to the topological classification, we note that the pairing function should be an eigenfunction of C_n in order to preserve the C_n symmetry in the superconducting phase (more precisely, to preserve the symmetry under the combination of C_n and a global phase rotation). Since C_n and C symmetries do not protect a nodal point or a nodal loop on the surface without time reversal symmetry, our discussion below is concentrated on the time-reversal-symmetric superconductors. To keep time reversal symmetry as well as C_n symmetry in the superconducting phase, the pairing function has a real eigenvalue under the G operation. Otherwise, the pairing function is not invariant under time reversal symmetry because time reversal changes the eigenvalue of the pairing function. Thus, it is enough to consider only even- or odd- C_n pairing $C_n \Delta(\mathbf{k}) C_n^{-1} = \pm \Delta(R_n \mathbf{k})$ for time-reversal-symmetric superconductors.

Throughout the classification, we assume that C_n commutes with T , i.e., $C_n T = T C_n$. It is satisfied in physically relevant systems such as nonmagnetic systems with finite/negligible spin-orbit coupling (class DIII with $C_n^m = -1$ and class CI with $C_n^m = 1$) and spin-polarized systems without spin-orbit coupling (class BDI with $C_n^m = 1$).

$(C_2 T)^2$	$(C_2 P)^2$	S^2	0D	1D
0	0	0	0	0
0	0	1	0	$\mathbb{Z}_{U(1)}$
1	1	1	\mathbb{Z}_2	\mathbb{Z}_2
1	-1	1	0	$\mathbb{Z}_{U(1)}$
-1	1	1	0	$2\mathbb{Z}_{U(1)}$
-1	-1	1	0	0

TABLE I. **Topological charges of gapless nodes at a generic momentum in the surface Brillouin zone.** C_2 is a twofold rotation around the surface normal axis. $C_{2z}T$, $C_{2z}P$, and S do not change crystal momentum, so they constrain the band topology and gap closing condition at generic momenta. $\mathbb{Z}_{U(1)}$ is the U(1) winding number carried by point nodes, 0D \mathbb{Z}_2 is the topological charge protecting line nodes, and 1D \mathbb{Z}_2 is the O(N) winding number that carried by a line node as a secondary topological charge [57].

A. Even- C_n (C_n -invariant) superconducting pairing

To study the protection of gapless states on the surface, we need to consider both C_n -invariant momenta and generic momenta. At generic momenta, there is no C_n -protected gapless point nodes for even- C_n pairing because C_n -related gapless states have the same U(1) winding number, so they are robust against breaking C_n symmetry as long as chiral symmetry is preserved and are thus not C_n -protected states. Therefore, only line nodes can appear as anomalous surface states at generic momenta. Since the 1D topological charge of line nodes is protected by rotational symmetries and is not the U(1) winding number protected by chiral symmetry [Table.I], line

nodes can appear as C_n -protected anomalous surface states.

As for the high-symmetry momenta, it is enough to analyze C_n -invariant momenta. For other high-symmetry momenta that are invariant under a subgroup of the C_n group, the representation of the subgroup at C_n -invariant momenta already captures the related topology. For example, let us consider the C_2 -invariant surface momenta $\bar{X} = (\pi, 0)$ and $\bar{Y} = (0, \pi)$ of a C_4 -symmetric system. The C_2 -protected higher-spin spectrum occurring at \bar{X} and \bar{Y} also occur at $\bar{\Gamma} = (0, 0)$ and $\bar{M} = (\pi, \pi)$. Since we consider strong topological phases that are robust against translation symmetry breaking that preserves C_n symmetry, we can consider a unit cell doubling along both x and y directions (such that four unit cells merge into a large unit cell). By this process, the higher-spin spectrum at \bar{X} and \bar{Y} are folded into the $\bar{\Gamma}$ point, but the strong topological phase does not change by definition. Therefore, the analysis of at the surface $\bar{\Gamma}$ point is enough to study the 3D strong topological phase protected by C_4 symmetry. We thus focus on the C_n -invariant line in the 3D Brillouin zone, the 1D winding number on which is responsible for the protection of the gapless states at the corresponding C_n -invariant momentum (as shown in the main text for C_2).

In the following, we first classify the higher-spin Majorana fermions at $\bar{\Gamma}$, i.e., classify 1D winding numbers along the line $(0, 0, k_z)$ in the 3D bulk Brillouin zone. The classification of the 1D winding numbers for two physically relevant classes of spin-orbit coupled systems and spin-SU(2)-symmetric systems were done in Ref. [59]. We extend this to other symmetry classes. After that, we identify symmetry classes that host doubly charged Majorana Fermi lines.

1. Chiral-symmetric systems without time reversal symmetry (class AIII)

Let us first forget about time reversal symmetry and consider C_n and chiral symmetries only. In the case of C_2 symmetry, we have two 1D invariants for each eigensector

$$\lambda \in \{\lambda_{\pm}\} = \begin{cases} \{-i, i\} & (C_2^2 = -1) \\ \{-1, 1\} & (C_2^2 = 1) \end{cases}.$$

Since $w = w_+ + w_-$ is total the winding number, which serves as the 1D topological invariant of the system and is protected by chiral symmetry, there remains only one 1D invariant relevant for the 3D topology protected by the simultaneous presence of C_2 and chiral symmetries. Similarly, there are two, three, and five crystalline 1D invariants for C_3 , C_4 , and C_6 symmetries because there are three eigenvalues for C_3

$$\lambda \in \{\lambda_{1\pm}, \lambda_2\} = \begin{cases} \{e^{\pm\pi i/3}, -1\} & (C_3^3 = -1) \\ \{e^{\pm 2\pi i/3}, 1\} & (C_3^3 = 1) \end{cases},$$

four eigenvalues for C_4

$$\begin{aligned} \lambda \in \{\lambda_{1\pm}, \lambda_{2\pm}\} &= \{e^{\pm\pi i/4}, e^{\pm 3\pi i/4}\} & (C_4^4 = -1) \\ \lambda \in \{\lambda_{1\pm}, \lambda_2, \lambda_3\} &= \{e^{\pm\pi i/2}, -1, 1\} & (C_4^4 = 1), \end{aligned} \quad (1)$$

AZ class	$(C_n)^n$	T^2	P^2	S^2	even- C_2	even- C_3	even- C_4	even- C_6	odd- $C_{n=2,6}$	odd- C_4	complex- C_n
DIII	-1	-1	1	1	$\mathbb{Z}_{U(1)} \times \mathbb{Z}_{\text{HS}}$	$\mathbb{Z}_{U(1)} \times \mathbb{Z}_{\text{HS}}$	$\mathbb{Z}_{U(1)} \times \mathbb{Z}_{\text{HS}}^2$	$\mathbb{Z}_{U(1)} \times \mathbb{Z}_{\text{HS}}^3$	$(\mathbb{Z}_2)_{\text{DC}}$	$(\mathbb{Z}_2)_{\text{M}}$	0
CI	-1	1	-1	1	$2\mathbb{Z}_{U(1)} \times \mathbb{Z}_{\text{HS}}$	$2\mathbb{Z}_{U(1)} \times \mathbb{Z}_{\text{HS}}$	$2\mathbb{Z}_{U(1)} \times \mathbb{Z}_{\text{HS}}^2$	$2\mathbb{Z}_{U(1)} \times \mathbb{Z}_{\text{HS}}^3$	0	0	0
CII	-1	-1	-1	1	$(\mathbb{Z}_2)_{\text{DC}}$	\mathbb{Z}_{HS}	$(\mathbb{Z}_2)_{\text{DC}} \times \mathbb{Z}_{\text{HS}}$	$(\mathbb{Z}_2)_{\text{DC}} \times \mathbb{Z}_{\text{HS}}^2$	$(\mathbb{Z}_2)_{\text{M}}$	$(\mathbb{Z}_2)_{\text{DC}}$	0
BDI	-1	1	1	1	0	\mathbb{Z}_{HS}	\mathbb{Z}_{HS}	\mathbb{Z}_{HS}^2	0	0	0
DIII	1	-1	1	1	$\mathbb{Z}_{U(1)}$	$\mathbb{Z}_{U(1)} \times \mathbb{Z}_{\text{HS}}$	$\mathbb{Z}_{U(1)} \times \mathbb{Z}_{\text{HS}}$	$\mathbb{Z}_{U(1)} \times \mathbb{Z}_{\text{HS}}^2$	0	0	0
CI	1	1	-1	1	$2\mathbb{Z}_{U(1)}$	$2\mathbb{Z}_{U(1)} \times \mathbb{Z}_{\text{HS}}$	$2\mathbb{Z}_{U(1)} \times \mathbb{Z}_{\text{HS}}$	$2\mathbb{Z}_{U(1)} \times \mathbb{Z}_{\text{HS}}^2$	0	0	0
CII	1	-1	-1	1	\mathbb{Z}_{HS}	\mathbb{Z}_{HS}	\mathbb{Z}_{HS}^2	\mathbb{Z}_{HS}^3	0	0	0
BDI	1	1	1	1	\mathbb{Z}_{HS}	\mathbb{Z}_{HS}	\mathbb{Z}_{HS}^2	\mathbb{Z}_{HS}^3	0	0	0
C or D	± 1	0	± 1	0	0	0	0	0	0	0	0
AIII	± 1	0	0	1	$\mathbb{Z}_{U(1)} \times \mathbb{Z}_{\text{HS}}$	$\mathbb{Z}_{U(1)} \times \mathbb{Z}_{\text{HS}}^2$	$\mathbb{Z}_{U(1)} \times \mathbb{Z}_{\text{HS}}^3$	$\mathbb{Z}_{U(1)} \times \mathbb{Z}_{\text{HS}}^5$	0	0	0

TABLE II. **Extended topological classification of C_n -symmetric 3D superconductors.** T , P , and S represent time reversal, particle-hole, and chiral symmetries used for Altland-Zirnbaur (AZ) symmetry classification. We assume $C_n T = T C_n$ and define T and P such that $TP = PT$. C_n and P satisfies the commutation relation $C_n P = \lambda P C_n$. Even- and odd- C_n correspond to $\lambda = +1$ and $\lambda = -1$, respectively, and complex- C_n indicate that λ is complex-valued. The subscript U(1) indicates that it is the 3D winding number of the Hamiltonian protected by chiral S symmetry. The subscripts HS, DC, and M indicate that they are responsible for the protection of higher-spin Majorana fermions (HSMFs), doubly charged Majorana Fermi lines (DCMFLs), and a C_n -multiplet of Majorana fermions (MMF), respectively, on the C_n -preserving surfaces. When time reversal symmetry is broken, there is no 3D topological superconductor protected by C_n symmetry. In class AIII, even-, odd-, and complex- C_n indicate the commutation relation $C_n S = \lambda S C_n$ instead of $C_n P = \lambda P C_n$.

and six eigenvalues for C_6

$$\begin{aligned} \lambda \in \{\lambda_{1\pm}, \lambda_{2\pm}, \lambda_{3\pm}\} &= \{e^{\pm\pi i/6}, e^{\pm\pi i/2}, e^{\pm5\pi i/6}\}, \\ \lambda \in \{\lambda_{1\pm}, \lambda_{2\pm}, \lambda_3, \lambda_4\} &= \{e^{\pm\pi i/3}, e^{\pm2\pi i/3}, -1, 1\}. \end{aligned} \quad (2)$$

for $C_6^6 = -1$ and $C_6^6 = 1$, respectively. Thus, in systems with C_n and S symmetries, we have

$$\begin{aligned} &\mathbb{Z}_{U(1)} \times \mathbb{Z}_{\text{HSF}} \text{ for } C_2, \\ &\mathbb{Z}_{U(1)} \times \mathbb{Z}_{\text{HSF}}^2 \text{ for } C_3, \\ &\mathbb{Z}_{U(1)} \times \mathbb{Z}_{\text{HSF}}^3 \text{ for } C_4, \\ &\mathbb{Z}_{U(1)} \times \mathbb{Z}_{\text{HSF}}^5 \text{ for } C_6, \end{aligned} \quad (3)$$

independent of the presence of spin-orbit coupling.

2. Constraints from time reversal symmetry

Let us now consider the effect of time reversal symmetry in chiral-symmetric systems, described by

$$\begin{aligned} w_{1D}^\lambda &= +(-1)^{s_T+s_C} w_{1D}^{\lambda*}, \\ w_{3D} &= -(-1)^{s_T+s_C} w_{3D}. \end{aligned} \quad (4)$$

which we derive in Methods in the main text. Here, s_T and s_C are defined by $T^2 = (-1)^{s_T}$ and $P^2 = (-1)^{s_C}$. First, time reversal symmetry can impose constraints on $\mathbb{Z}_{U(1)}$: it is always trivial when the AZ class is BDI or CII where $T^2 = P^2$. Also, in class CI, we have $2\mathbb{Z}_{U(1)}$ instead of $\mathbb{Z}_{U(1)}$ because spinless time reversal symmetry forbids an odd 3D winding number, as shown in Methods in the main text. Second, the C_n -protected invariants \mathbb{Z}_{HSF} depends on whether the representation satisfies $(C_n)^n = 1$ or -1 . We explicitly count the number of constraints on the \mathbb{Z}_{HSF} invariants from time reversal symmetry below.

3. AZ classes DIII and CI

In spin-orbit coupled systems and spin-SU(2)-symmetric systems, the AZ class is DIII and CI, respectively. For spin-orbit coupled systems, where $(C_n)^n = -1$, time reversal symmetry constraints are

$$w_+ + w_- = 0, \quad (5)$$

for C_2 eigensectors

$$\begin{aligned} w_+ + w_- &= 0, \\ w_0 &= 0 \end{aligned} \quad (6)$$

for C_3 eigensectors,

$$\begin{aligned} w_{1+} + w_{1-} &= 0, \\ w_{2+} + w_{2-} &= 0 \end{aligned} \quad (7)$$

for C_4 eigensectors, and

$$\begin{aligned} w_{1+} + w_{1-} &= 0, \\ w_{2+} + w_{2-} &= 0, \\ w_{3+} + w_{3-} &= 0 \end{aligned} \quad (8)$$

for C_6 eigensectors. Here, we do not count the constraint on the total winding number $w = \sum_i w_i$, because it is irrelevant for the 3D topological phase. Thus, by the zero, one, one, and two constraints on $C_{n=2,3,4,6}$ eigensectors from time reversal symmetry, the topological classification is reduced to

$$\begin{aligned} &\mathbb{Z}_{U(1)} \times \mathbb{Z}_{\text{HSF}} \text{ for } C_2, \\ &\mathbb{Z}_{U(1)} \times \mathbb{Z}_{\text{HSF}} \text{ for } C_3, \\ &\mathbb{Z}_{U(1)} \times \mathbb{Z}_{\text{HSF}}^2 \text{ for } C_4, \\ &\mathbb{Z}_{U(1)} \times \mathbb{Z}_{\text{HSF}}^3 \text{ for } C_6. \end{aligned} \quad (9)$$

For spin-SU(2)-rotation-symmetric systems, where $(C_n)^n = 1$,

$$\begin{aligned} w_+ &= 0, \\ w_- &= 0, \end{aligned} \quad (10)$$

for C_2 eigensectors

$$\begin{aligned} w_+ + w_- &= 0, \\ w_0 &= 0 \end{aligned} \quad (11)$$

for C_3 eigensectors, and

$$\begin{aligned} w_{1+} + w_{1-} &= 0, \\ w_2 &= 0, \\ w_3 &= 0 \end{aligned} \quad (12)$$

for C_4 eigensectors, and

$$\begin{aligned} w_{1+} + w_{1-} &= 0, \\ w_{2+} + w_{2-} &= 0, \\ w_3 &= 0, \\ w_4 &= 0 \end{aligned} \quad (13)$$

for C_6 eigensectors. Again, the constraint $w = 0$ on the total 1D winding number does not affect the classification of 3D topological phases. Thus, we have a classification

$$\begin{aligned} 2\mathbb{Z}_{U(1)} &\text{ for } C_2, \\ 2\mathbb{Z}_{U(1)} \times \mathbb{Z}_{\text{HSF}} &\text{ for } C_3, \\ 2\mathbb{Z}_{U(1)} \times \mathbb{Z}_{\text{HSF}} &\text{ for } C_4, \\ 2\mathbb{Z}_{U(1)} \times \mathbb{Z}_{\text{HSF}}^2 &\text{ for } C_6. \end{aligned} \quad (14)$$

We can also obtain a classification for the class CI systems with $(C_n)^n = -1$ and the class DIII systems with $(C_n)^n = 1$ although their relation to physical systems is not clear. The classifications are respectively

$$\begin{aligned} 2\mathbb{Z}_{U(1)} \times \mathbb{Z}_{\text{HSF}} &\text{ for } C_2, \\ 2\mathbb{Z}_{U(1)} \times \mathbb{Z}_{\text{HSF}} &\text{ for } C_3, \\ 2\mathbb{Z}_{U(1)} \times \mathbb{Z}_{\text{HSF}}^2 &\text{ for } C_4, \\ 2\mathbb{Z}_{U(1)} \times \mathbb{Z}_{\text{HSF}}^3 &\text{ for } C_6, \end{aligned} \quad (15)$$

and

$$\begin{aligned} \mathbb{Z}_{U(1)} &\text{ for } C_2, \\ \mathbb{Z}_{U(1)} \times \mathbb{Z}_{\text{HSF}} &\text{ for } C_3, \\ \mathbb{Z}_{U(1)} \times \mathbb{Z}_{\text{HSF}} &\text{ for } C_4, \\ \mathbb{Z}_{U(1)} \times \mathbb{Z}_{\text{HSF}}^2 &\text{ for } C_6. \end{aligned} \quad (16)$$

4. AZ classes BDI and CII

In spin-polarized systems without spin-orbit coupling, although time reversal and spin-rotation symmetries are broken

separately, the combination of time reversal and a π -rotation of spin (around the axis perpendicular to the magnetic order) defines an effective time reversal satisfying $T^2 = 1$, so the AZ class is BDI. Also, a spinless representation of rotation operators is possible because spin and orbital degrees of freedom are independent, i.e., $(C_n)^n = 1$. In this case, time reversal symmetry constraints on the 1D winding numbers are none for C_2 eigensectors,

$$w_+ - w_- = 0 \quad (17)$$

for C_3 eigensectors,

$$w_{1+} - w_{1-} = 0 \quad (18)$$

for C_4 eigensectors and

$$\begin{aligned} w_{1+} - w_{1-} &= 0, \\ w_{2+} - w_{2-} &= 0 \end{aligned} \quad (19)$$

for C_6 eigensectors. Time reversal symmetry also imposes that the 3D winding number vanishes. Furthermore, we should not forget, in addition to these time reversal symmetry constraints, that the total 1D winding number $w = \sum_i w_i$ is not relevant for the 3D topology. Thus,

$$\begin{aligned} \mathbb{Z}_{\text{HSF}} &\text{ for } C_2, \\ \mathbb{Z}_{\text{HSF}} &\text{ for } C_3, \\ \mathbb{Z}_{\text{HSF}}^2 &\text{ for } C_4, \\ \mathbb{Z}_{\text{HSF}}^3 &\text{ for } C_6. \end{aligned} \quad (20)$$

For completeness, we also consider $(C_n)^n = -1$ in the class BDI. We have constraints

$$w_+ - w_- = 0. \quad (21)$$

for C_2 eigensectors

$$w_+ - w_- = 0 \quad (22)$$

for C_3 eigensectors,

$$\begin{aligned} w_{1+} - w_{1-} &= 0, \\ w_{2+} - w_{2-} &= 0 \end{aligned} \quad (23)$$

for C_4 eigensectors and

$$\begin{aligned} w_{1+} - w_{1-} &= 0, \\ w_{2+} - w_{2-} &= 0, \\ w_{3+} - w_{3-} &= 0 \end{aligned} \quad (24)$$

for C_6 eigensectors. Thus,

$$\begin{aligned} 0 &\text{ for } C_2, \\ \mathbb{Z}_{\text{HSF}} &\text{ for } C_3, \\ \mathbb{Z}_{\text{HSF}} &\text{ for } C_4, \\ \mathbb{Z}_{\text{HSF}}^2 &\text{ for } C_6. \end{aligned} \quad (25)$$

Similarly, for class CII systems with $(C_n)^n = 1$ and $C_n = -1$, we have

$$\begin{aligned} \mathbb{Z}_{\text{HSF}} & \text{ for } C_2, \\ \mathbb{Z}_{\text{HSF}} & \text{ for } C_3, \\ \mathbb{Z}_{\text{HSF}}^2 & \text{ for } C_4, \\ \mathbb{Z}_{\text{HSF}}^3 & \text{ for } C_6. \end{aligned} \quad (26)$$

and

$$\begin{aligned} 0 & \text{ for } C_2, \\ \mathbb{Z}_{\text{HSF}} & \text{ for } C_3, \\ \mathbb{Z}_{\text{HSF}} & \text{ for } C_4, \\ \mathbb{Z}_{\text{HSF}}^2 & \text{ for } C_6, \end{aligned} \quad (27)$$

respectively.

5. Doubly charged Majorana Fermi lines

As shown in the main text, a single doubly charged Majorana Fermi lines can appear when $T^2 = -1$ and $(C_2T)^2 = (C_2P)^2 = 1$ are satisfied ($T^2 = 1$ excludes the presence of a single doubly charged Majorana Fermi line). In the case of even- C_n pairing, the only possibility is to have $T^2 = C_2^2 = P^2 = -1$ since we assume $C_nT = TC_n$. Let us show that there exists a doubly charged Majorana Fermi line in this symmetry class. We consider the following Majorana Hamiltonian

$$H_0 = k_x \sigma_x + k_y \tau_z \sigma_y. \quad (28)$$

It has symmetries under $C_{2z} = i\tau_z \sigma_z$, $T = i\sigma_y K$, $P = i\tau_y K$, which satisfy $T^2 = C_2^2 = P^2 = -1$. Perturbations that respect these symmetries are

$$\delta H = m_1 \tau_y \sigma_x + m_2 \tau_z, \quad (29)$$

where $m_{1,2}(-\mathbf{k}) = m_{1,2}(\mathbf{k})$. Nonzero $m_{1,2}$ deforms the fourfold degenerate point to a line node, as one can see from the spectrum of

$$H = H_0 + \delta H, \quad (30)$$

which is

$$E = \pm \sqrt{k_x^2 + k_y^2} \pm \sqrt{m_1^2 + m_2^2}. \quad (31)$$

It shows that the gap closes at $E = 0$ when $k_x^2 + k_y^2 = m_1^2 + m_2^2$, which forms a loop generically. The Hamiltonian H respects $C_{n=2,4,6}$ symmetry with even- C_n pairing where

$$C_{n=2,4,6} = e^{-i\frac{\pi}{n}\tau_z \sigma_z}. \quad (32)$$

C_n symmetry requires that $m_{1,2}(R_n \mathbf{k}) = m_{1,2}(\mathbf{k})$.

B. Odd- $C_{2,6}$ superconducting pairing

Let us note that odd- C_6 pairing is even- C_3 . In this case, C_3 eigensectors have well-defined 1D winding numbers although we cannot assign the 1D winding number for C_6 eigensectors since C_6 and S do not commute. However, C_6 symmetry imposes that two sectors with eigenvalues λ and $-\lambda$, which has the same C_3 eigenvalue, has zero winding number. Moreover, since the odd- $C_{2,6}$ pairing also forbids a nontrivial 3D winding number, the only possibility is to have Majorana fermions at generic momenta with a trivial total winding number.

For odd- $C_{2,6}$ pairing, the surface can always be gapped when $C_2^2 = 1$ because C_2 operator itself can serve as a mass term. To see this, we note that C_2 is a Hermitian matrix because it is a unitary matrix satisfying $C_2^2 = 1$, and it has the same symmetry property as the Hamiltonian, i.e., $(C_2T)C_2(C_2T)^{-1} = C_2$, $(C_2P)C_2(C_2P)^{-1} = -C_2$, and $(C_n)C_2(C_n)^{-1} = C_2$. We thus consider the cases with $C_2^2 = -1$ only.

1. Doubly charged Majorana Fermi lines

A single doubly charged Majorana Fermi line can appear when $T^2 = -1$ and $(C_2T)^2 = (C_2P)^2 = 1$. This condition is satisfied only when $T^2 = C_2^2 = -1$ and $P^2 = 1$ for odd- $C_{2,6}$ pairing, which is the case of spin-orbit coupled systems we treat in the main text. The low-energy Hamiltonian takes the form

$$H = k_x \tau_z \sigma_x + k_y \tau_z \sigma_y + \mu \tau_z + \Delta(\mathbf{k}) \tau_x \sigma_z, \quad (33)$$

where μ is the chemical potential, and $\Delta(-\mathbf{k}) = -\Delta(\mathbf{k})$. It is symmetric under $C_2 = i\tau_z \sigma_z$, $T = i\sigma_y K$, and $P = \tau_y \sigma_y K$. If we require $C_6 = \tau_z e^{-i\frac{\pi}{6}\sigma_z}$ symmetry, an additional constraint $\Delta(R_6 \mathbf{k}) = -\Delta(\mathbf{k})$ is imposed.

2. Doublet and sextet of Majorana fermions

Table I shows that point nodes at generic momenta can be protected when $(C_2T)^2 = 1$ and $(C_2P)^2 = -1$, or $(C_2T)^2 = -1$ and $(C_2P)^2 = 1$. As we show below, rotation-protected Majorana fermions can appear in the former case, whereas they do not appear in the latter case.

Let us first consider the former case. Since we consider odd- $C_{2,6}$ pairing with $C_2^2 = -1$, we have $T^2 = P^2 = -1$. We again introduce

$$H_0 = k_x \sigma_x + k_y \tau_z \sigma_y. \quad (34)$$

Here, we take $T = i\sigma_y K$, $P = i\tau_y K$. Then, two possible C_2 representations are $C_2 = -i\sigma_z$ and $C_2 = -i\tau_x \sigma_y$. Those two representations are equivalent because they are related by a unitary transformation of the basis by $U = e^{-i\frac{\pi}{4}\tau_x \sigma_x}$. We take $C_2 = -i\sigma_z$. Then, symmetry-allowed perturbations are

$$\delta H = m_1(\mathbf{k}) \tau_x \sigma_y + m_2(\mathbf{k}) \tau_y \sigma_z + m_3(\mathbf{k}) \tau_x + m_4(\mathbf{k}) \tau_z, \quad (35)$$

where $m_1(-\mathbf{k}) = -m_1(\mathbf{k})$, and $m_{2,3,4}(-\mathbf{k}) = m_{2,3,4}(\mathbf{k})$. The m_1 term anticommutes with H_0 , but it does not open the gap because it vanishes at $\mathbf{k} = 0$. The other terms are not mass terms, so they also do not open the gap. Instead, δH splits the fourfold degeneracy at $\mathbf{k} = 0$ into a doublet of Majorana fermions. If we require $C_6 = \tau_z e^{-i\frac{\pi}{6}\tau_z\sigma_z}$ symmetry, $m_1(R_6\mathbf{k}) = -m_1(\mathbf{k})$, $m_{2,3}(\mathbf{k}) = 0$, and $m_4(R_6\mathbf{k}) = m_4(\mathbf{k})$. Then, a sextet of Majorana fermions appear at generic momenta by perturbations.

Next, we consider $(C_2T)^2 = -1$ and $(C_2P)^2 = 1$. Since $(C_2T)^2 = -1$, C_2T symmetry imposes Kramers degeneracy at each momentum, so the minimal Majorana Hamiltonian needs four bands and takes the form $H_{\min} = \rho_0 \otimes (k_x\sigma_x + k_y\sigma_y)$, where ρ_0 is the 2×2 identity matrix. It has $C_2T = i\rho_y\sigma_xK$ and $C_2P = \rho_y\sigma_yK$ symmetries. The Majorana fermion described by this Hamiltonian carries the $U(1)$ winding number two. Let us overlap two such Majorana fermions with opposite winding numbers to see whether a rotation-protected gapless spectrum can appear. Its Hamiltonian has a 8×8 form

$$H_0 = k_x\sigma_x + k_y\tau_z\sigma_y. \quad (36)$$

There are four mass terms preserving $C_2T = i\rho_y\sigma_xK$ and $C_2P = i\rho_y\sigma_yK$ symmetries, which are

$$\delta H_{\text{mass}} = (m_1\tau_x + m_2\tau_y\rho_x + m_3\tau_y\rho_y + m_4\tau_y\rho_z) \otimes \sigma_y, \quad (37)$$

where $m_{1,2,3,4}$ are constants.

We note that C_2 symmetry cannot forbid all mass terms. If we require that C_2 symmetry disallows all mass terms, C_2 anticommutes with the mass terms as well as H_0 . Then, C_2 should be proportional to the chiral operator $S = \sigma_z$, but $C_2 \propto S$ is incompatible with the odd- C_2 pairing condition. Since C_2 anticommutes with $S = \sigma_z$ and H_0 , it should be either $C_2 = -i\tau_y\sigma_y$, $C_2 = -i\tau_x\rho_i\sigma_y$ for any $i = x, y, z$, or $C_2 = -i\tau_x\sigma_y$.

Let us now show that C_6 symmetry also cannot forbid all mass terms. When $C_2 = -i\tau_y\sigma_y$, C_2 symmetry imposes $m_1 = 0$, and the mass term has the form $\delta H_{\text{mass}} = (m_2\rho_x + m_3\rho_y + m_4\rho_z)C_2$. In order for C_6 to eliminate δH_{mass} , C_3 should act nontrivially on all Pauli matrices $\rho_{i=x,y,z}$ (C_2 acts trivially by definition). However, it is impossible because a C_3 rotation leaves at least one dimension invariant in the three-dimensional ρ_i space: the largest irreducible representation is two-dimensional, and the one-dimensional representation is trivial. Thus, there exists a C_6 -invariant mass term. We can analyze the case with $C_2 = -i\tau_x\rho_{i=x,y,z}\sigma_y$ in a similar way. We choose $i = x$ for simplicity, but it is straightforward to consider other choices. We have $m_2 = 0$ due to C_2 symmetry, and $\delta H_{\text{mass}} = (m_1\rho_x + m_3\tau_z\rho_z + m_4\tau_z\rho_y)C_2$. As in the previous case for ρ_i s, $\sigma_1 \equiv \rho_x$, $\sigma_2 \equiv \tau_z\rho_z$, and $\sigma_3 \equiv \tau_z\rho_y$ satisfy the Lie algebra of Pauli matrices, $[\sigma_i, \sigma_j] = 2i\epsilon_{ijk}\sigma_k$. Again C_2 do not act on these Pauli matrices, and C_3 leaves at least one Pauli matrix invariant, so a mass term is allowed. Finally, when $C_2 = -i\tau_x\sigma_y$, the mass term im_1C_2 is invariant under C_6 . Thus, in all cases, the spectrum can be gapped in a way that respects C_6 symmetry and other internal symmetries T and S .

C. Odd- C_4 superconducting pairing

As in the odd- C_6 pairing case, the only possibility is to have Majorana fermions at generic momenta with a trivial total winding number. Odd- C_4 pairing is even- C_2 , but a higher-spin spectrum cannot be protected because C_4 trivializes the 1D winding number in each C_2 eigensector. Also, odd- C_4 symmetry forbids a nontrivial 3D winding number. The anomalous surface states can thus appear as a quartet of Majorana fermions with zero total $U(1)$ winding number or as a doubly charged Majorana Fermi line.

1. Doubly charged Majorana Fermi lines

A single doubly charged Majorana Fermi line can appear when $C_2^2 = T^2 = P^2 = -1$ for odd- C_4 pairing. This case is treated in the analysis of even- C_2 pairing above. The only thing to check is whether it is compatible with C_4 symmetry. One can see that the Hamiltonian Eq. (30) and symmetry representations $C_{2z} = i\tau_z\sigma_z$, $T = i\sigma_yK$, $P = i\tau_yK$ are compatible with $C_4 = \tau_z e^{-i\frac{\pi}{4}\tau_z\sigma_z}$.

2. Quartet of Majorana fermions

As we show in the main text, a quartet of Majorana fermions can be protected by C_4 symmetry in the same way as in rotation-protected topological crystalline insulators. They are characterized by the $(\mathbb{Z}_2)_M$ invariant.

Such a quartet of Majorana fermions can be protected only in the spin-orbit coupled systems ($C_4^4 = T^2 = -1$ and $P^2 = 1$). A point node at generic momenta can be protected when either $(C_2T)^2 = 1$ and $(C_2P)^2 = -1$ or $(C_2T)^2 = -1$ and $(C_2P)^2 = 1$ [Table. I]. In the former, the system is either spin-orbit coupled system or spin- $SU(2)$ -symmetric system ($(C_n)^n = T^2 = 1$ and $P^2 = -1$). Since a d -wave pairing in two-dimensional spin- $SU(2)$ -symmetric systems produces four Majorana fermions in lattice systems, we know that there is no anomaly associated with the existence of four Majorana fermions.

$(C_2T)^2 = -1$ and $(C_2P)^2 = 1$ with odd- C_4 pairing can be realized in exotic systems satisfying either $C_4^4 = -1$, $T^2 = 1$ and $P^2 = 1$ or $C_4^4 = 1$, $T^2 = -1$ and $P^2 = 1$. In these cases, C_2T symmetry imposes Kramers degeneracy at every momenta on the C_4 -invariant surface, and a stable Majorana point node has fourfold degenerate zero mode and carries an even number of winding number. It is nontrivial to see whether a quartet of these Majorana fermions can be protected by crystalline symmetry. Let us thus explicitly write down the low-energy effective Hamiltonian.

We first consider $C_{2z}T = i\sigma_yK$ and $C_{2z}P = K$ symmetries. The most general form of the fourband Hamiltonian is $H(\mathbf{k}) = f_1(\mathbf{k})\rho_y\sigma_x + f_2(\mathbf{k})\rho_y\sigma_z$. We take $f_1 = k_x$, $f_2 = k_y$ to describe a Majorana fermion. It has winding number two. Let us construct an eightband Hamiltonian describing an overlap of two Majorana fermions with opposite winding numbers,

which is

$$H_0 = k_x \rho_y \sigma_x + k_y \tau_z \rho_y \sigma_z. \quad (38)$$

Here, τ is the Pauli matrix for the flavor degrees of freedom. $C_{2z}T$ - and $C_{2z}P$ -preserving mass terms are

$$\delta H = m_1 \tau_x \rho_y \sigma_z + m_2 \tau_y \rho_z \sigma_x + m_3 \tau_y \rho_x \sigma_x + m_4 \tau_y \sigma_z. \quad (39)$$

Let us now see whether C_{4z} that anticommutes with the particle-hole operator can exclude all mass terms. A possible representation for C_{2z} is a linear combination of elements in $\{1, \tau_z\} \otimes \{\rho_x, \rho_z, \rho_y \sigma_y\}$ when $C_{2z}^2 = 1$ and in $i\tau_y \otimes \{\rho_x, \rho_z, \rho_y \sigma_y\} \cup \{i\sigma_y\}$ when $C_{2z}^2 = -1$, if we require that $C_{2z}H_0(\mathbf{k})C_{2z}^{-1} = H(-\mathbf{k})$ and commutes with both $C_{2z}T$ and $C_{2z}P$. Here, we can choose ρ_x from $\{\rho_x, \rho_z, \rho_y \sigma_y\}$ by a transform of basis without affecting the form of H_0 and δH . To see this, let us note that $\Gamma_1 = \rho_x, \Gamma_2 = \rho_z, \Gamma_3 = \rho_y \sigma_x, \Gamma_4 = \rho_y \sigma_y, \Gamma_5 = \rho_y \sigma_z$ form five mutually anticommuting 4×4 matrices. Since $\{\rho_x, \rho_z, \rho_y \sigma_y\} = \{\Gamma_1, \Gamma_2, \Gamma_4\}$, we can rotate them fixing $\Gamma_3 = \rho_y \sigma_x$ and $\Gamma_5 = \rho_y \sigma_z$ (consider a $SO(2)$ rotation in a three-dimensional space with Γ_1, Γ_2 , and Γ_4 as basis). It leaves H_0 invariant, and the form of δH is preserved after a redefinition of m_2, m_3, m_4 . Thus, we have without loss of generality that $C_{2z} = \rho_x$ or $\tau_z \rho_x$ when $C_{2z}^2 = 1$ [?] and $C_{2z} = i\tau_y \rho_x$ when $C_{2z}^2 = -1$ (we do not consider $C_{2z} = i\sigma_y = iS$ because it is inconsistent with the assumption of odd- C_{4z} pairing).

Let us see there are no protected surface states. When $C_{2z} = \rho_x$, we have $m_1 = m_2 = 0$. Let us write the remaining mass term as $\delta H = \tau_y \rho_x \sigma_x (m_3 - im_4 \rho_x \sigma_y)$ and note that $\rho_x \sigma_y = C_{2z}S$ anticommutes with C_{4z} . Since the C_{4z} transformation of a mass term should be a mass term (because conjugating with C_{4z} does not change the commutation relation), the only possibility is that either the m_3 term or the m_4 term is invariant under C_{4z} . When $C_{2z} = \tau_z \rho_x$, $\delta H = \tau_x \rho_x \sigma_z (m_1 + m_2 C_{2z}S)$, and the same conclusion is derived. When $C_{2z} = i\tau_y \rho_x$, there exists a unique choice $C_{4z} = \tau_z \rho_y \sigma_z e^{-i\frac{\pi}{4}\tau_y \rho_x}$ that eliminates all the mass terms if we forget about symmetry of H_0 . This choice is, however, inconsistent with C_{4z} symmetry of H_0 .

II. A MODEL OF SPIN-POLARIZED C_2 -PROTECTED TOPOLOGICAL SUPERCONDUCTOR

Here we construct a model of spin-polarized C_2 -protected topological superconductor hosting a spin-3/2 fermion on the surface. This system belongs to the class $C_2^2 = T^2 = P^2 = 1$.

We consider the following normal-state Hamiltonian.

$$h = \mu + f_1 \rho_y \sigma_x + f_2 \sigma_y + f_3 \sigma_z + m_1 \rho_z + m_2 \rho_z \sigma_z, \quad (40)$$

where $f_1 = \sin k_x$, $f_2 = \sin k_y$, and $f_3 = 2 - \cos k_x - \cos k_y - \cos k_z$. It is symmetric under $C_{2z} = \mathcal{I} = \sigma_z$ and $\mathcal{T} = K$: $C_{2z}h(\mathbf{k})(C_{2z})^{-1} = h(-k_x, -k_y, k_z)$, $\mathcal{I}h(\mathbf{k})\mathcal{I}^{-1} = h(-\mathbf{k})$, $\mathcal{T}h(\mathbf{k})\mathcal{T}^{-1} = h(-\mathbf{k})$. This Hamiltonian describes two Dirac points carrying nontrivial \mathbb{Z}_2 monopole charges at

$k_z = \pm\pi/2$ when $m_1 = m_2 = 0$, and the Dirac points become nodal lines with a finite size when $m_1, m_2 \neq 0$ [73, 74]. We open the bulk superconducting gap fully by introducing even- C_2 pairing $\Delta(\mathbf{k}) = -i\Delta \sin k_z$. When $|\mu|$, $|m_1|$, and $|m_2|$ are small, this pairing introduces winding number $+1$ (-1) for each band within the $C_2 = +1$ (-1) sector along the $(k_x, k_y, k_z) = (0, 0, k_z)$ line. Note that our normal state Hamiltonian and pairing function are both diagonal along this line. The winding number of the sector with $\rho_z = s_\rho = \pm 1$ and $\sigma_z = s_\sigma = \pm 1$ is given by the phase winding number of $E_{\rho\sigma}(\mathbf{k}) + \Delta_{\rho\sigma}(\mathbf{k}) = \mu + s_\rho m_1 + s_\rho s_\sigma m_2 - s_\sigma \cos k_z - i\Delta \sin k_z$, which is just s_σ when $|\mu|$, $|m_1|$, $|m_2|$ are much smaller than one. So, we have $w_{\text{rot}} = 2$, while $w_{\text{rot}} = 0$ for other C_2 -invariant lines because no Fermi surface is there. We show the numerically calculated spectrum for $\mu = -0.2$, $m_1 = m_2 = 0.2$, and $\Delta = 1$ in Fig. 1, where one can observe the anomalous surface state with a fourfold degenerate crossing point at $(k_x, k_y) = (0, 0)$.

Let us comment on the previous work on two-dimensional spin-3/2 fermions in the literature. About a decade ago, four spin-3/2 fermions called *birefringent fermions* (described by a variant of Eq. (40)) were shown to appear in the Brillouin zone of a 2D square optical lattice [50]. This seems like indicating that a non-superconducting (and non-anomalous) realization of spin-3/2 fermions is possible in two dimensions. However, those birefringent fermions are not strictly protected by the symmetry of ordinary complex fermionic (i.e., non-Majorana) systems. Our analysis shows that their topological protection requires sublattice symmetry (=chiral symmetry), which is present only in nearest-neighbor hopping models, as well as C_2 and T symmetries. Therefore, to our knowledge, the Majorana fermion proposed here is the first as well as anomalous realization of a symmetry-protected birefringent fermion in two dimensions.

III. NUMERICAL CALCULATION OF TOPOLOGICAL CHARGE OF SURFACE STATES IN ROTATION-PROTECTED TOPOLOGICAL INSULATORS

In the main text, we show that C_n -protected surface states of the Fang-Fu type [19] (a C_n -multiplet of Dirac/Majorana fermions) are characterized by the topological invariant Q_n . To confirm this further, let us consider a lattice model of C_2 -

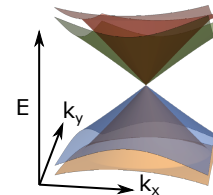


FIG. 1. **Surface spectrum of a spin-polarized C_2 -protected topological superconductor.** We use the model in Eq. (40) with $\mu = -0.2$, $m_1 = m_2 = 0.2$, and $\Delta = 1$. The system has 20 unit cells along the z direction and periodic boundary condition along the xy direction.

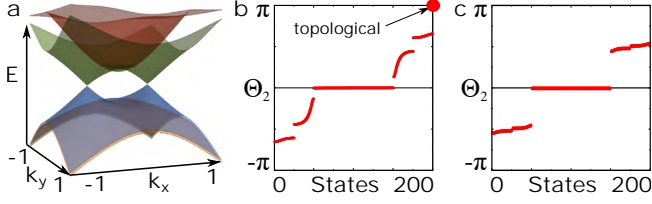


FIG. 2. **C_2 -protected topological crystalline insulator.** The system has a finite number — 20 in **a** and 50 in **b** and **c** — of unit cells along z with open boundaries, while it is periodic along x and y . **a**. Low-energy surface spectrum near $(k_x, k_y) = (0, 0)$. **b** and **c**. C_2 -Wilson line spectrum for the whole system with 200 occupied bands. They are calculated over an π -arc of the circle $k_x^2 + k_y^2 = 1$ in **b**, enclosing two Dirac points, and $k_x^2 + k_y^2 = 0.3^2$ in **c**, enclosing no Dirac points. Anomalous gapless states on each of the top and bottom surfaces give the eigenvalue $\Theta_2 = \pi$ when the circle encloses them, such that the whole system has two eigenstates with $\Theta_2 = \pi$. Thus, $Q_2 = e^{i\Theta_2} = -1$ on the circle $k_x^2 + k_y^2 = 1$ for each of the top and bottom surfaces.

protected topological crystalline insulator. We begin with a strong topological insulator protected by time reversal symmetry.

$$H_{\pm}^{\text{STI}} = \sin k_x \rho_x \sigma_x \pm \sin k_y \rho_y \sigma_y + \sin k_z \rho_z \sigma_z + (2 - \cos k_x - \cos k_y - \cos k_z) \rho_z, \quad (41)$$

where $\rho_{i=x,y,z}$ and $\sigma_{i=x,y,z}$ are Pauli matrices for the orbital and spin degrees of freedom. This system has symmetries under $\mathcal{T} = i\sigma_y K$, $\mathcal{C}_{2z} = -i\sigma_z$, and $\mathcal{I} = \rho_z$. It has one Dirac cone on each surface whose chirality depending on the sign \pm . From this we construct the Hamiltonian of a C_2 -protected topological insulator as

$$H = H_+^{\text{STI}} \oplus H_-^{\text{STI}}. \quad (42)$$

Let us preserve $\mathcal{C}_{2z} = (-i\sigma_z) \oplus (-i\sigma_z)$ symmetry of this system by adding C_{2z} - and T -preserving perturbations (we also keep P symmetry for convenience of analysis below)

$$\delta H = m_1 \tau_x \rho_z + m_2 \tau_z \rho_z + m_3 \tau_x + m_4 \tau_z \quad (43)$$

to the Hamiltonian H , where $\tau_{i=x,y,z}$ are Pauli matrices for the chirality degrees of freedom $+$ and $-$. Then, we have two Dirac cones on each C_2 -preserving surface as shown in Fig. 2(a).

Since our choice of C_{2z} has the same representations for the two surface Dirac cones with opposite chirality, the rotation-protected topological charge Q_n is nontrivial as shown in Methods in the main text. To see this numerically, we take the open boundary condition along z and the periodic boundary condition along x and y . Then we calculate the spectrum Θ_2 of the C_2 -Wilson line around an π -arc on the circle $|\mathbf{k}| = 1$ from $\theta = 0$ to $\theta = \pi$ for the whole system. Figure 2(b) shows that there appears two eigenstates of the C_2 -Wilson line with $\theta_2 = \pi$. Since the bulk is gapped, this nontrivial value should be attributed to the gapless surface states. One is from the top surface, and the other is from the bottom surface because of inversion symmetry. Thus, we conclude that $Q_2 = 1 \pmod{2}$ for each of the top and bottom surface states.

IV. CLASSIFICATION OF PAIRING FUNCTIONS IN DIRAC SEMIMETAL AND NODAL LINE SEMIMETAL MODELS

We consider two lattice models in the main text. One is a Dirac semimetal with gap-opening terms. It is

$$h_1 = -\mu + f_1 \rho_z + f_2 \rho_x \sigma_z + f_3 \rho_y + f_4 \rho_x \sigma_x + f_5 \rho_x \sigma_y, \quad (44)$$

where $\rho_{i=x,y,z}$ and $\sigma_{i=x,y,z}$ are Pauli matrices for orbital and spin degrees of freedom, respectively, and $f_1 = 4 - 2(\cos k_x + \cos k_y) - \cos k_z$, $f_2 = \sin k_x$, $f_3 = -\sin k_y$, $f_4 = 3 \sin k_z (\cos k_y - \cos k_x) + m_0 \sin k_z$, and $f_5 = -\sin k_z \sin k_x \sin k_y + m_1 \sin k_z$. m_0 and m_1 are gap-opening terms that break C_{4z} , M_x , M_{x+y} , and M_y symmetries. When $m_0 = m_1 = 0$, h_1 has T and D_{4h} symmetries under

$$\begin{aligned} \mathcal{T} &= i\sigma_y K, \\ \mathcal{M}_x &= i\sigma_x, \\ \mathcal{M}_y &= i\rho_z \sigma_y, \\ \mathcal{M}_{x+y} &= \frac{1}{\sqrt{2}}(\sigma_x - \rho_z \sigma_y), \\ \mathcal{M}_z &= i\sigma_z, \\ \mathcal{C}_{4z} &= e^{-i(\pi/4)(2\rho_0 - \rho_z)s_z}. \end{aligned} \quad (45)$$

We classify superconducting pairing functions based on their transformation properties under D_{4h} symmetry group operations in Tables. III and IV.

As we state in the main text, $\Delta(\mathbf{k}) = \Delta_{1a'} \sin k_z = \Delta_e \sin k_z \sigma_z$ is the unique even- C_{2z} pairing function that leads to a rotation-protected topological superconductor. Let us explain why it is so. They are Δ_{1a} , Δ_{1b} , Δ_2 , Δ_3 in Table III, and $\Delta_{1a'} \sin k_z$, $\Delta_{1b'} \sin k_z$, $\Delta_{2'} \sin k_z$, $\Delta_{3'} \sin k_z$ from Table IV if we consider the lowest Fourier expansions in k_z (we neglect $\sin k_x$ and $\sin k_y$ terms because they vanish at C_{2z} -invariant lines). Δ_2 , Δ_3 , $\Delta_{2'} \sin k_z$ and $\Delta_{3'} \sin k_z$ are odd- C_{4z} pairing, so they are also incompatible with higher-spin Majorana fermions. Δ_{1a} and Δ_{1b} are even-parity pairing, so they are incompatible with higher-spin Majorana fermions as we discuss in the main text. The only remaining are $\Delta_{1a'} \sin k_z$ and $\Delta_{1b'} \sin k_z$, which has the same symmetry properties. However, the latter leads to a topologically trivial phase at the C_4 -invariant line, and in fact, it does not open the bulk gap.

The other model describes a nodal line semimetal gapped by spin-orbit coupling. The Hamiltonian is

$$\begin{aligned} h_2 &= -\mu + \sin k_z \rho_y + (M - \sum_{i=x,y,z} \cos k_i) \rho_z \\ &+ \lambda_{\text{SO}} (\sin k_x \rho_x \sigma_y - \sin k_y \rho_y \sigma_x), \end{aligned} \quad (46)$$

which is symmetric under

$$\begin{aligned}
\mathcal{T} &= i\sigma_y K, \\
\mathcal{M}_x &= i\sigma_x, \\
\mathcal{M}_y &= i\sigma_y, \\
\mathcal{M}_{x+y} &= \frac{i}{\sqrt{2}}(\sigma_x + \sigma_y), \\
\mathcal{M}_z &= i\rho_z \sigma_z, \\
\mathcal{C}_{4z} &= e^{-i\frac{\pi}{4}\sigma_z}.
\end{aligned} \tag{47}$$

Superconducting pairing functions are classified according to transformation properties under D_{4h} symmetry group operations in Tables. V, and VI.

Let us note that not every odd- C_{4z} pairing gives a quartet of Majorana fermions on the C_{4z} -invariant surface. We show in the main text that a d-wave pairing $\Delta_2(\cos k_y - \cos k_x) + \Delta_3 \sin k_x \sin k_y$ gives the quartet of Majorana fermions. In contrast, other odd- C_4 pairing $k_x \Delta_{4a'} + k_y \Delta_{4b'}$ or $k_x \Delta_{5a'} + k_y \Delta_{5b'}$ opens the full gap on the C_{4z} -invariant surface.

Δ	Matrix	Irrep	C_4	M_z	M_x	M_y	M_{x+y}
Δ_{1a}	$\rho_0\sigma_0$	A_{1g}	+	+	+	+	+
Δ_{1b}	$\rho_z\sigma_0$	A_{1g}	+	+	+	+	+
Δ_2	$\rho_y\sigma_y$	B_{1u}	-	-	-	-	-
Δ_3	$\rho_y\sigma_x$	B_{2u}	-	-	+	+	+
Δ_{4a}	$\rho_x\sigma_0$	E_u	$-\Delta_{4b}$	+	+	-	$-\Delta_{4b}$
Δ_{4b}	$\rho_y\sigma_z$	E_u	Δ_{4a}	+	-	+	$-\Delta_{4a}$

TABLE III. Time-reversal-preserving constant pairing functions of the Dirac semimetal h_1 .

Δ	Matrix	Irrep	C_4	M_z	M_x	M_y	M_{x+y}
$\Delta_{1a'}$	$\rho_0\sigma_z$	A_{2g}	+	+	-	-	-
$\Delta_{1b'}$	$\rho_z\sigma_z$	A_{2g}	+	+	-	-	-
$\Delta_{2'}$	$\rho_x\sigma_y$	B_{1u}	-	-	-	-	-
$\Delta_{3'}$	$\rho_x\sigma_x$	B_{2u}	-	-	+	+	+
$\Delta_{4a'}$	$\rho_0\sigma_y$	E_g	$-\Delta_{4b'}$	-	-	+	$-\Delta_{4b'}$
$\Delta_{4b'}$	$\rho_z\sigma_x$	E_g	$\Delta_{4a'}$	-	+	-	$-\Delta_{4a'}$
$\Delta_{5a'}$	$\rho_z\sigma_y$	E_g	$-\Delta_{5b'}$	-	-	+	$-\Delta_{5b'}$
$\Delta_{5b'}$	$\rho_0\sigma_x$	E_g	$\Delta_{5a'}$	-	+	-	$-\Delta_{5a'}$
$\Delta_{6a'}$	$\rho_y\sigma_0$	E_u	$-\Delta_{6b'}$	+	+	-	$-\Delta_{6b'}$
$\Delta_{6b'}$	$-\rho_x\sigma_z$	E_u	$\Delta_{6a'}$	+	-	+	$-\Delta_{6a'}$

TABLE IV. Time-reversal-breaking constant pairing functions of the Dirac semimetal h_1 . These constant pairing functions should be multiplied by a k-odd function to preserve time reversal symmetry.

Δ	Matrix	Irrep	C_4	M_z	M_x	M_y	M_{x+y}
Δ_{1a}	$\rho_0\sigma_0$	A_{1g}	+	+	+	+	+
Δ_{1b}	$\rho_z\sigma_0$	A_{1g}	+	+	+	+	+
Δ_2	$\rho_y\sigma_z$	A_{1u}	+	-	-	-	+
Δ_3	$\rho_x\sigma_0$	A_{2u}	+	-	+	+	-
Δ_{4a}	$\rho_y\sigma_y$	E_u	$-\Delta_{4a}$	+	-	+	Δ_{4b}
Δ_{4b}	$\rho_y\sigma_x$	E_u	Δ_{4b}	+	+	-	Δ_{4a}

TABLE V. Time-reversal-preserving constant pairing functions of the gapped nodal line semimetal model described by h_2 .

Δ	Matrix	Irrep	C_4	M_z	M_x	M_y	M_{x+y}
$\Delta_{1a'}$	$\rho_0\sigma_z$	A_{2g}	+	+	-	-	-
$\Delta_{1b'}$	$\rho_z\sigma_z$	A_{2g}	+	+	-	-	-
$\Delta_{2'}$	$\rho_x\sigma_z$	A_{1u}	+	-	-	-	-
$\Delta_{3'}$	$\rho_y\sigma_0$	A_{2u}	+	-	+	+	+
$\Delta_{4a'}$	$\rho_0\sigma_y$	E_g	$-\Delta_{4b'}$	-	-	+	$\Delta_{4b'}$
$\Delta_{4b'}$	$\rho_0\sigma_x$	E_g	$\Delta_{4a'}$	-	+	-	$\Delta_{4a'}$
$\Delta_{5a'}$	$\rho_z\sigma_y$	E_g	$-\Delta_{5b'}$	-	-	+	$\Delta_{5b'}$
$\Delta_{5b'}$	$\rho_z\sigma_x$	E_g	$\Delta_{5a'}$	-	+	-	$\Delta_{5a'}$
$\Delta_{6a'}$	$\rho_x\sigma_y$	E_u	$-\Delta_{6b'}$	+	-	+	$\Delta_{6b'}$
$\Delta_{6b'}$	$\rho_x\sigma_x$	E_u	$\Delta_{6a'}$	+	+	-	$\Delta_{6a'}$

TABLE VI. Time-reversal-breaking constant pairing functions of the gapped nodal line semimetal model described by h_2 . These constant pairing functions should be multiplied by a k-odd function to preserve time reversal symmetry.